REPORT DOCUMENTATION PAGE

Form Approved
OMB No. 0704-0188

1. REPORT DATE *(DD-MM-YYYY)*	**2. REPORT TYPE**	**3. DATES COVERED** *(From - To)*
05-06-2009		

4. TITLE AND SUBTITLE
Using Biomechanical Optimization to Interpret Dancers' Pose Selection for a Partnered Spin

5a. CONTRACT NUMBER

5b. GRANT NUMBER

5c. PROGRAM ELEMENT NUMBER

6. AUTHOR(S)

Selbach-Allen, Megan E. (Megan Elise), 1986-

5d. PROJECT NUMBER

5e. TASK NUMBER

5f. WORK UNIT NUMBER

7. PERFORMING ORGANIZATION NAME(S) AND ADDRESS(ES)

8. PERFORMING ORGANIZATION REPORT NUMBER

9. SPONSORING / MONITORING AGENCY NAME(S) AND ADDRESS(ES)
U.S. Naval Academy
Annapolis, MD 21402

10. SPONSOR/MONITOR'S ACRONYM(S)

11. SPONSOR/MONITOR'S REPORT NUMBER(S)
Trident Scholar Project Report no. 382 (2009)

12. DISTRIBUTION / AVAILABILITY STATEMENT

This document has been approved for public release; its distribution is UNLIMITED

13. SUPPLEMENTARY NOTES

14. ABSTRACT

Our goal was to determine whether expert swing dancers physically optimize their pose for a partnered spin. In a partnered spin, two dancers connect hands and spin around a single vertical axis. We describe the pose of a couple by the angles of their joints in a two-dimensional plane. These angles were outputs of an optimization model that gave the ideal pose for a couple. A biomechanical model built in Mathematica allowed comparisons to live dancers with the use of a motion capture system.

15. SUBJECT TERMS
Nonlinear optimization, biomechanics, motion capture, swing dance

16. SECURITY CLASSIFICATION OF:			**17. LIMITATION OF ABSTRACT**	**18. NUMBER OF PAGES**	**19a. NAME OF RESPONSIBLE PERSON**
a. REPORT	**b. ABSTRACT**	**c. THIS PAGE**		93	**19b. TELEPHONE NUMBER** *(include area code)*

Standard Form 298 (Rev. 8-98)
Prescribed by ANSI Std. Z39.18

Using Biomechanical Optimization to Interpret Dancers' Pose Selection for a Partnered Spin

Megan E. Selbach-Allen

May 6, 2009

Abstract

Our goal was to determine whether expert swing dancers physically optimize their pose for a partnered spin. In a partnered spin, two dancers connect hands and spin around a single vertical axis. We describe the pose of a couple by the angles of their joints in a two-dimensional plane. These angles were outputs of an optimization model that gave the ideal pose for a couple. A biomechanical model built in Mathematica allowed comparisons to live dancers with the use of a motion capture system.

The optimization objective is to maximize angular acceleration, by minimizing the resistance to spin, but still producing torque. The model considers only external forces and neglects internal forces. It consists of equations derived from physical principles such as Newton's laws and moment of inertia calculations that govern how people move. Using numerical non-linear optimization we found the pose for each couple that maximizes their angular acceleration. Different dancers are differently sized, so every couple has a different optimal pose. Each couple's optimal pose was compared to the pose they actually assumed for the spin.

Our motion capture system consisted of four video cameras, reflective balls that could be tracked, and software to integrate the different angles of the cameras. The captured data consisted of the three-dimensional location of each of the marked body joints. We used this data to determine the angles of the joints to calculate the couple's actual pose. The couple's actual pose was used to calculate a predicted angular acceleration. This predicted acceleration was then compared to the optimal acceleration to determine a fraction of optimal for each couple. We hypothesized that expert swing dancers would achieve a higher fraction of their optimal acceleration than beginners. While difference between expert and beginners was not significant our results for optimal poses were intuitively logical.

Keywords: nonlinear optimization, biomechanics, motion capture

Acknowledgements

My research this year would not have been possible without the assistance of a number of people. First and foremost I would like to thank my advisors Professor Sommer Gentry and Professor Kevin McIlhany for your constant support and suggestions for when I got stuck. You challenged, encouraged, and supported me throughout the year.

Next I would like to thank the Trident Committee as a whole for the time and effort you put in to making this program a success. This unique opportunity would not be possible without the time that you put in to making the program work. Additionally, I would like to specifically thank Professor Carl Wick, the Director for student research for organizing everything for us this year and ensuring that we kept on track.

My project also would not have been possible without people willing to take their free time and let me record their dancing. I have to acknowledge all of the dancers who participated in my project from Charm City Swing in Baltimore and the Swing Dance Club at the US Naval Academy. I appreciate your willingness to let me turn the cameras on you and for dancing the same steps over and over.

My year has also involved a number of administrative hurdles that Mrs. Joyce Fletcher, the Math Department secretary has helped me overcome. I know I created a lot of extra work for you, but you were always patient with me and I appreciate everything you have done. Additionally Jeff Walbert and the physics machine shop helped me with constructing my calibration structure. I am very grateful for your assistance.

Finally, I would like to thank my parents for their support over the year. Thank you for lending a listening ear as I unloaded on you, and thank you for the laptop, which has been a lifesaver this year. I would not be in the place I am today without your support this year and for the past 23 years.

Contents

List of Figures

List of Tables

Chapter 1

Why swing dance and physics?

1.1 The Rhythm Circle

This work began with a question of whether expert lindy hop swing dancers use physics to perform a rhythm circle in the most optimal way. To answer this question, we built a mathematical model to represent the pose dancers would choose to maximize his or her ability to spin quickly.

Lindy Hop is a fast paced style of dancing that originated in the 1920s and is now danced recreationally and competitively. Swing dance is an American folk partner dance form that originated in the Harlem of the 1920's and 1930's. Today this dance has developed into quite an athletic endeavor. Lindy Hop is danced to very fast music and can involve aerial tricks in addition to fancy footwork. To reach a level of competitive expertise, advanced dancers often train intensely for five to ten years before reaching the top levels of competition.

A rhythm circle is a movement where a couple spins as a unit around a single vertical axis. A good rhythm circle would look smooth, but also involve the dancers rotating fast. When discussing this movement, dancers often talk about minimizing moment of inertia or the need to create torque to spin, however, no one has actually studied this movement and determined quantitatively if they do what they claim in their discussions of physics. While no one has undertaken a study of swing dance in this style, extensive work has been done with motion capture and sports. A description of relevant articles related to this work is provided in Chapter 2. Figure 1.1 shows a couple in the midst of a Lindy move.

Figure 1.1: Swing dancing is enjoyed recreationally by millions of people around the country.

1.2 What to optimize?

The goal of this work is to determine if dancers optimize a physical objective when performing a partnered spin. We created a notation system of letter variables and a series of equations that model the dancers' pose. The notation system is fully explained in Chapter 3. With this notation, we developed a few candidate mathematical objectives for describing the best pose.

The actual value of the objective will vary for each couple because it will be determined by their individual sizes. We considered moment of inertia, angular acceleration, and angular velocity all as possible objectives that better dancers might minimize or maximize. Minimizing the moment of inertia was the simplest objective function that we considered. We did extensive work with this objective by first defining all the distances to the axis of rotation in terms of joint angles and body measurements in Chapter 3 and then calculating moments of inertia as described in Chapter 5. We added constraints, described in Chapter 4, to account for the realities of the human body that did not allow the person to enter a position that would be physically impossible.

Inertia was ultimately rejected as an objective function because it yields a simple answer that we know does not describe the correct pose. Since our performance metric

is having the dancers spin as fast as possible without tripping or falling over; the ideal objective would be to maximize angular velocity. However, we determined this value would be too difficult to model based on parameters we could measure. Instead, we maximized the angular acceleration. This value was easier to calculate, and because angular acceleration is what allows the couples to reach their max speeds it still has a correlation to maximizing speed. Finally, this value takes into account the need to produce force from the feet along with the need to minimize moment of inertia, which we already calculated.

We created a model to calculate the torques the dancers create to propel themselves in a circle, along with their moments of inertia. Determining the torques involved was a challenge. Instead of directly calculating torque, we used a surrogate method for estimating the external forces acting on the dancer. Our method for calculating torque is explained in Chapter 6.

1.3 Simplifying Assumptions

We made a number of simplifying assumptions in our analysis. First, we neglected internal forces that the person might generate in a chosen pose. This assumption made it easier to solve the problem, as we have no method for measuring the internal forces exerted by the dancers. The methods for determining internal forces are extremely complex and beyond the scope of this research [4].

The true spinning motion that dancers create when performing a rhythm circle is very complex because the velocity is constantly varying with the interactions of friction and the foot pushing to create acceleration. We assumed that dancers' poses were fixed and did not change over the course of the spin, even though in reality the dancers do change their position, for example as they take steps. While we acknowledge that the feet moving changes the pose, we observed that the overall pose of the dancers remains relatively stable.

Another simplification we made concerned the connection between the two dancers. In reality the dancers have multiple points of connection: leader's right hand around follower's left shoulder blade, follower's left hand on leader's right shoulder, the couple's arms touching, and leader's left hand holding the follower's right hand. To focus on the spinning motion, we summed these forces and considered them as if they acted at a single connecting point located between the couple.

In fact, the dancers accelerate by pushing off the floor and slow down when they are not pushing due to friction. This interplay eventually reaches an equilibrium where rotational velocity is relatively constant. We did not consider these two phases

of the spin in our model. Instead we focused on maximizing angular acceleration. If a couple accelerates faster they will reach a higher rotational velocity than a couple with lower angular acceleration.

1.4 The Optimization scheme

We used a numerical optimization scheme to find a pose that maximized angular acceleration for each couple. The problem is nonlinear because of the presence of trigonometric functions relating the joint angles, which determine the pose, to the objective function. In order to track our equations and perform numerical optimization we used Mathematica. Mathematica has an "NMaximize" function that implements a global non-linear optimization scheme. The optimization problem was particularly challenging because not only was it non-linear, but it was very high dimensional. Our decision variables were the 14 angles that defined the couple's pose. The objective was to minimize our function estimating moment of inertia, or to maximize our function estimating rotational acceleration, see Chapter 6.

1.5 Dancing to Verify

We used a motion capture system to record live dancers performing the rhythm circle. The MaxTraq 3d motion capture system by Innovision Systems is made up of four video cameras and nineteen reflective markers that are placed on each dancer. A full description of this system is presented in Chapter 8. The system records the X-Y-Z location of each of the points 32 times a second. Using this data we determined dancers' actual joint angles for their chosen pose.

In order to determine how close each couple was to their calculated optimum position, we had to create a metric for comparison. The metric used the joint angles from the actual pose the dancers held, and input the values into the model to determine an achieved angular acceleration. To determine each couple's fraction of their optimal acceleration, we calculated the ratio of their achieved acceleration to their optimal acceleration. These fractions were then compared using a Mann-Whitney statistical test. Chapter 9 describes our process for data analysis. We hypothesized that experienced dancers would find a pose closer to their optimum than novice dancers, and thus reach a statistically significant higher fraction of their theoretically achievable acceleration.

Chapter 2

What's been done: Previous work in human motion and optimization

2.1 Studies in Motion and Biomechanics

2.1.1 Dogs Optimization

Obviously dogs do not study calculus to learn to calculate derivatives or solve equations. However, Pennings demonstrated that even without doing calculations the dogs chose a near optimal path for when to stop running and jump in the water and swim in order to minimize the time required to reach a ball floating in the waters of Lake Michigan [9]. This article is relevant because it demonstrates an example in which animals with no knowledge of calculus acted in an optimal way. We are attempting to determine if dancers, many with a minimal knowledge of math and physics, still use these principles naturally in attempting to spin as fast as possible.

2.2 Human Motion Study

2.2.1 In Competitive Sports

Many studies on competitive athletes show that particular human movements seem to be optimal according to some objective. For example, Raasch et al. found good agreement between an optimal control model of maximum speed bicycle pedaling and actual human pedaling strategy [2]. In this study researchers showed that athletes

maximized the power produced in a pedal stroke by pushing on the down stroke and pulling on the up stroke.

In another study of optimized human motion, Yeadon [14] looked at the optimized performance of a straight arm backward longswing on the still rings in mens artistic gymnastics. Because gymnasts lose points for excessive swing at the beginning or conclusion of the swing, Laws attempted to minimize swing through realistic changes in technique. They began with an actual performance, and then allowed variance from that performance in their model as it searched for the optimal positions. One distinction is that they began with an actual performance and used that as the basis for their search. Yeadon determined that with timing within 15ms, gymnasts can minimize their excess swing down to two degrees.

2.2.2 In Dance

Kenneth Laws has shown that the quality of the jumps, spins, and lifts individual dancers perform is dependent on how well the dancers exploit their own physical characteristics along with using the laws of physics [6]. In one study he examined different aspects of momentum transfer within dance [5]. His work included the use of the arms to increase the height of a jump and the use of the "windup" leg in correctly performing pirouette and fouette turns. These studies and other like them imply that human beings unconsciously use physical and mathematical principles when they execute complicated movements. While extensive studies have been conducted on single person optimal motion, partnered motion has rarely been addressed because of the complexity of dealing with two people coordinating their actions.

2.3 Coordination in Partnered Motion

When two people accomplish a task together, such as dancing, they work together and much of their communication is nonverbal and channeled through their physical contact. For example, a male dancer leads his partner by increasing or letting off pressure on the females shoulder blade to communicate his intent to move her backward or forward. The vast majority of their communication is non-verbal. According to Gentry [3] expert swing dancers have a common vocabulary of movements from which they choose and then the leader communicates his choice to the follower who then receives the signals and then performs the movement. In this way they dance together.

When two individuals perform a task together, their need to coordinate creates an

extra complication, so one cannot automatically predict whether they will be more efficient together than an individual working alone. This principle was demonstrated by Kyle Reed when he had individuals perform a task and then had them perform the same task together. A clear correlation between the effectiveness of the individuals vise the effectiveness of the two people working together did not exist.

We will work with movements in which the coordination problem can be largely ignored without significantly affecting the results. The problem of understanding the physical principles of multiple human motions is sufficiently different from the single person case without considering coordination and will contribute to the current body of knowledge.

2.4 Animation and Optimization

Finally, our work may relate to computer animation. Using the insight that human beings often move unconsciously in optimal patterns, programmers are able to develop simpler algorithms to represent the motions. Safonova et al. used optimization to animate a character in lower dimensional space [12]. Because they were able to represent the character's in lower dimensional space, the animation was much smaller in size and required significantly less computer time to render. Because of the decreased dimensionality of the space, the character's motions were simplified but they still resembled the actual human movements. This observation supports the prediction that human beings move in an optimal, logical pattern. Our work deals with simplified poses, but as [12] shows simplification can be done and still allow realistic modeling of the movements when people are moving in an optimal way.

2.5 Body Modeling

2.5.1 Building the Body

In his study involving gymnasts on the rings, Yeadon developed a body model composed of truncated cones and cylinders [14]. The trunk of the person is treated as two connected stadiums, truncated cones, and the arms and legs are modeled with cylinders. His model has since been used extensively because it represents the body with a relatively high degree of accuracy, but still provides for regular shapes that can be used in mathematical modeling. Other researchers have elaborated on how to calculate parameters for the Yeadon body model [8]. To simplify the calculations we

developed our model using only cylinders.

While he did not build a unique model like Yeadon, Hatze attempted to synthesize the work done on body modeling into a single paper [4]. His work showed that to build an effective model one must consider the purpose of the model to determine the amount of detail that is necessary. If one wants to model a piano player, one would build a model with more degrees of freedom and detail in the hands. Conversely, in our model we do not put any detail into the hands because we are interested in major joint angles of the body pose.

Hatze also looked at attempts to model the interior dynamic muscle contractions. He claimed that attempts to model the muscle contractions were generally lacking because they were not able to account for enough of the major variables. In our model we ignored the internal muscular forces.

2.5.2 Center of Mass and Force Calculations

Our understanding of how people could be treated as rigid bodies with definite forces acting through their center of mass came from Tozeren [13]. One of his examples calculates the location of the center of mass of a complex body by breaking it into parts and computing a weighted average of the center of mass of each of the body parts.

Tozeren's book also explained concepts such as the moment of inertia of an object and how to use vectors to define how a force was acting on an object. Interestingly, all of Tozeren's examples were of individual movements, not partnered movements. His text did, however, provide valuable insight into the physics of the human body.

2.5.3 Weight Distribution

To determine the distribution of the dancers' weight throughout the different parts of their body we relied on a study by Nikolova and Toshev on the Bulgarian population [7]. In their study they calculated the average size, weight distribution, center of mass, and moments of inertia of Bulgarians. Their system for segmenting the body was very similar to our method, so we used the results to partition each dancer's weight among body segments. Dancer's total weight was self-reported.

2.5.4 Biomechanics and Robotics

The study of biomechanics, including moments of inertia and their effects on human motion was first developed in the 1940s to improve the unsatisfactory prosthetic devices available to amputees. Biomechanics is the application of engineering principles to animal and human movement problems. Current applications of human motion analysis include developing robots with human-like characteristics. QRIO, a robot developed by Sony, is able to recover from being pushed backward. In order to program QRIO to react properly, the developers studied how humans react to regain a balanced center of mass. Conversely, the robot must be programmed to put itself off balance at times in order to take a step forward. If it were to remain in a balanced position all the time, it would not move anywhere. This insight was gained through studies of people walking.

Similarly we will study how people move interactively, which may provide insights to programmers attempting to design robots to work together or in tandem with humans. In a call for papers published this past year, the Naval Research Office offered more support to people working on the problem of collaborative motion [1]. The long-term developments of this work might include battlefield robots that can act as medics working together to transport wounded soldiers.

Chapter 3

Jointed Body Model Development

3.1 The Stick: the Simplest Model

Our simplest mathematical model for the rhythm circle represents the dancers as two single thin rods. As you can see in Figure 3.1, the body is represented by lines whose length is the height of the person, and the pose is determined by angle of the body measured from the horizon. In this model the length of the arms is fixed. The only other parameter is the height of the dancer. Additionally, the only decision variable is the angle of the dancers' body with the ground. While this model did not present a very detailed picture of the pose, it provided a basis from which to build our understanding of the problem. The challenge presented by this model was how to calculate the moment of inertia of a tilted thin rod. This calculation involved defining the moment of inertia with an equation to represent the varying distance to the axis of rotation along the length of the body. The calculations for the moment of inertia of a single thin rod, explained in Chapter 5, were simpler than for a jointed 3-dimensional representation.

3.2 The Stick with a Hip

In addition to the components present in the original model, the bend at the hip was added as a decision variable. The angle at the hip was still modeled as the angle from the horizon to the torso on the side of the hip closest to the axis of rotation. This model is illustrated in Figure 3.2. Because even a bent stick is not a realistic depiction of a human body, and not very interesting as a model because of

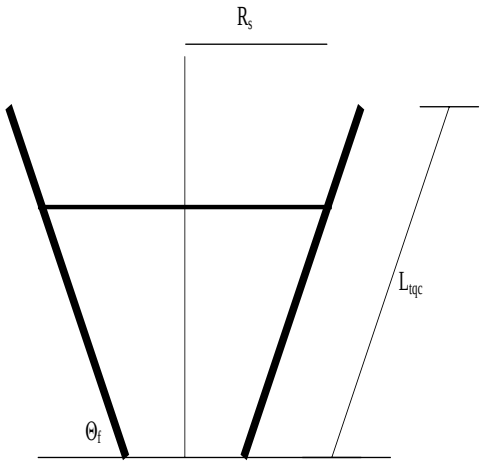

Figure 3.1: The most basic model we considered with the dancers represented as rigid rods. R_s is the range to the shoulder from the axis of rotation, L_tqc is the height of the person and θ is the angle at which the dancers are standing.

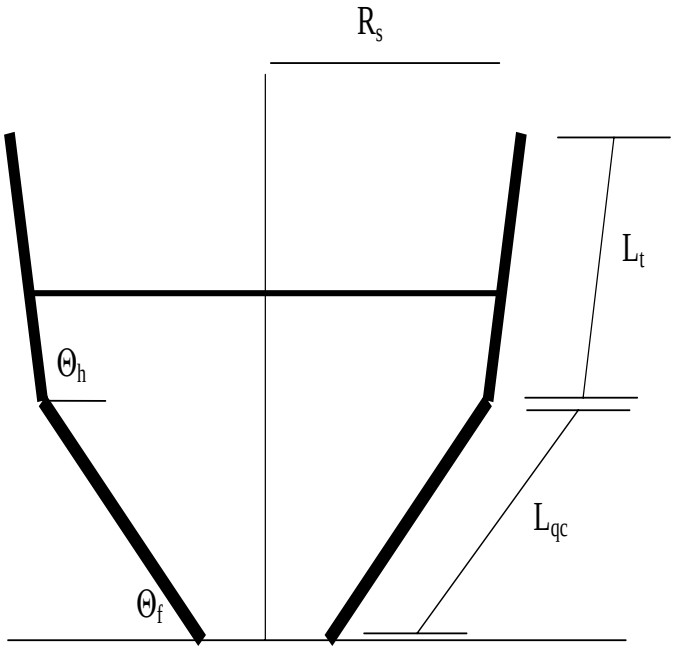

Figure 3.2: Stick Figures with a hip joint. The abbreviations are the same as 3.1 with the addition of a hip angle, θ_h and the splitting of the body into two sections representing the torso and the legs.

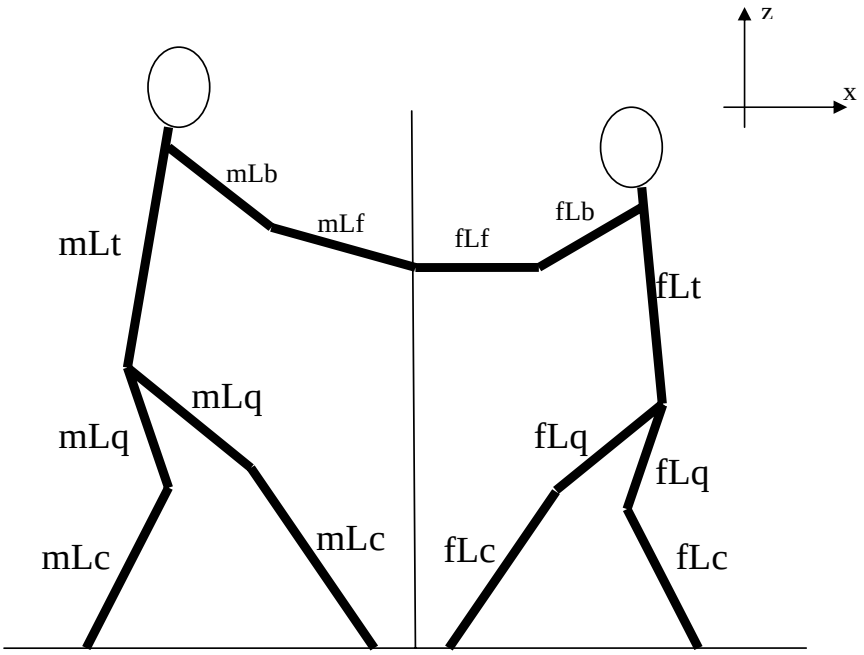

Figure 3.3: Developed model with each of the lengths notated.

its simplicity, we advanced the model so that it included seven angles for each person and separate parameters for each of their body parts. While the full model is not a perfect representation of the freedom of movements available, it should have enough detail to produce interesting information about dancer pose selection.

3.3 Full Model Notation

Figure 3.3 shows the stick diagram with lengths labeled. The f and m represent whether the dancer is the leader or follower, while the L denotes that the value is the length of a body part. The final letter in each of the variables denotes which specific part of the body that variable represents. Table 3.1 provides a full explanation of the what each of the variables mean.

These values were used extensively in the calculations for moment of inertia, location of the center of mass, and value of the torques involved in the spin.

Likewise Figure 3.4 illustrates how we defined the angles for our fully developed model. The angles of different joints with the horizon were the only decision variables in our optimization problem and how we defined the dancer's pose. Table 3.3 fully

Lengths	
mLf	Length of forearms of leader
mLb	Length of biceps of leader
mLt	Length of torso of leader
mLq	Length of upper leg (quads) of leader
mLc	Length of lower leg (calf) of leader
fLf	Length of forearms of follower
fLb	Length of biceps of follower
fLt	Length of torso of follower
fLq	Length of upper leg (quads) of follower
fLc	Length of lower leg (calf) of follower

Table 3.1: Table of the notation we used to describe the dancers bodies.

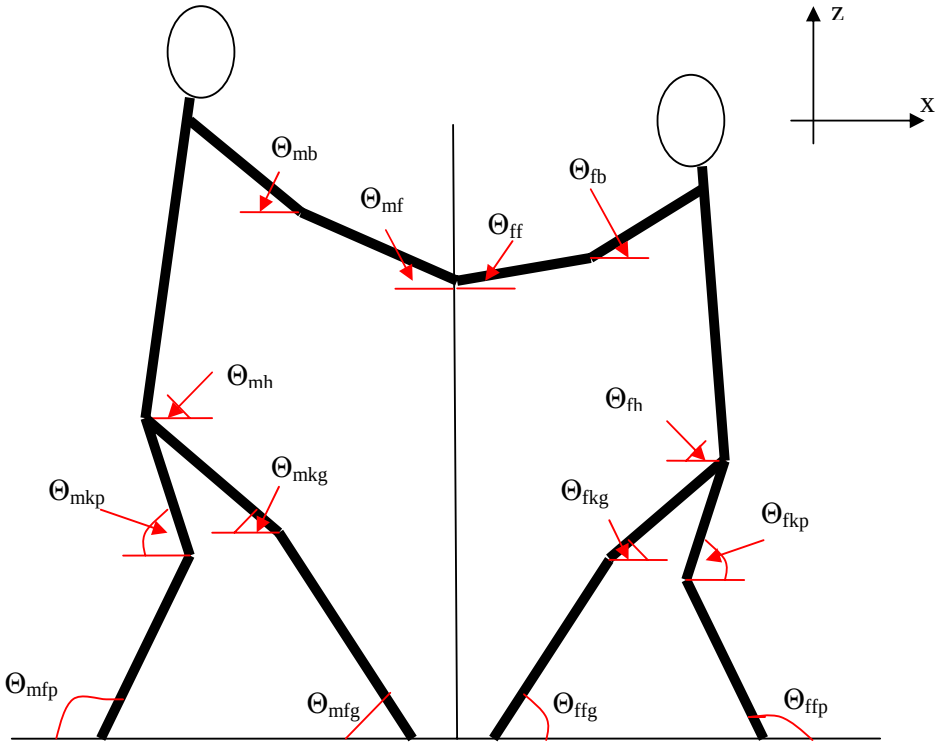

Figure 3.4: Developed model with the angles notated. Each dancer is defined by seven joint angles.

Angles			
θ_{mf}	Angle of Forearms	$-\pi/4$	$\pi/2$
θ_{mb}	Angle of Biceps	0	$\pi/2$
θ_{mh}	Angle of Hip	$\pi/4$	$3*\pi/4$
θ_{mkg}	Angle of Knee Grind	0	θ_{mfg}
θ_{mkp}	Angle of Knee Push	0	θ_{mfp}
θ_{mfg}	Angle of Foot Grind	0	π
θ_{mfp}	Angle of Foot Push	0	π
θ_{ff}	Angle of Forearms	$-\pi/4$	$\pi/2$
θ_{fb}	Angle of Biceps	0	$\pi/2$
θ_{fh}	Angle of Hip	$\pi/4$	$3*\pi/4$
θ_{fkg}	Angle of Knee Grind	0	θ_{ffg}
θ_{fkp}	Angle of Knee Push	0	θ_{ffp}
θ_{ffg}	Angle of Foot Grind	0	π
θ_{ffp}	Angle of Foot Push	0	π

Table 3.2: Angle notation with upper and lower bounds

explains the label for each angle. Also, the table mentions starting values that we used to begin the optimization process.

The m and f that appear in Figure 3.3 and Figure 3.4 distinguish between the male and female dancers, which we also used to distinguish between the leader and the follower. While not all male dancers are leaders and not all female dancers are followers, we chose to make this distinction for simplicity.

Also, one might notice in Table 3.3 the labeling "push" and "grind". These words were used to distinguish between the two legs. When we originally discussed the problem with two feet and viewed videos of dancers we determined that one of the feet stayed closer to the axis of rotation and was mainly used for balance and did not contribute to the spin, but it countered the spin by "grinding" on the floor. The other leg was further from the axis of rotation and was used to "push" the dancer around the circle and thus we labeled each foot the push foot and grind foot.

We used trigonometry to calculate the distance from each point on the body to the axis of rotation based on the pose and the parameters for each couple. The hands were assumed to be at the axis of rotation, defined as zero. From that point the rest of the body was defined. A full description of the variables used to represent the distance to the axis of rotation for each joint in the body follows in the next chapter and is illustrated in Table 3.3.

3.4 Fully Developed Model

The fully developed model should allow for the realistic representation of a couple. While the motion of this model is confined to the two-dimensional plane, it can be described in thee-dimensional space as a collection of cylinders. Because we moved into using cylinders, calculating the moment of inertia for this model was more complicated than the models that represented the dancers as thin rods. More explanation of the moment of inertia calculations follows in chapter 5.

3.5 Defining Distances

Each distance from the axis of rotation, the z-axis, to the locations of the body's joints was labeled R and had a subscript denoting a part of the body. The body parts were labeled subscript e for elbow, s for shoulder, h for hip, kg and kp for knee grind and knee push, and finally fg and fp for foot grind and foot push. The lengths of each piece, L, and angles to the horizon, θ, were similarly labeled with subscripts. For example, the distance from the elbow to the axis of rotation was defined as $R_e = L_f * Cos[\theta_f]$. The distance to the shoulder is based on the length of the upper arm and the distance to the elbow, $R_s = L_b * Cos[\theta_b] + R_e$. All other distances are calculated based on the distances to the body joints calculated before it. Therefore the distances between each of the feet and the axis of rotation is determined by the length parameters of the person and the angles of his pose. Table 3.3 shows our notation for the distances to the axis of rotation.

3.6 Body Radius Definition

When the model was made to be three-dimensional with cylinders instead of two-dimensional, an additional parameter, the radius of the individual body parts, needed to be defined. We treated each of the body parts as a cylinder with a constant radius. The radius of the torso was defined as the distance from the middle of the neck to the shoulder. Table 3.4 gives variable names used to represent the radius of each body part.

Distance Labels	
mRe	distance from leader elbow to z-axis
mRs	distance from leader shoulder to z-axis
mRh	distance from leader hip to z-axis
$mRkp$	distance from leader push knee to z-axis
$mRkg$	distance from leader grind knee to z-axis
$mRfp$	distance from leader push foot to z-axis
$mRfg$	distance from leader grind foot to z-axis
fRe	distance from follower elbow to z-axis
fRs	distance from follower shoulder to z-axis
fRh	distance from follower hip to z-axis
$fRkp$	distance from follower push knee to z-axis
$fRkg$	distance from follower grind knee to z-axis
$fRfp$	distance from follower push foot to z-axis
$fRfg$	distance from follower grind foot to z-axis

Table 3.3: Notation for the distances to each dancer's joints from the axis of rotation.

Body Radius Notation	
mrt	radius of leader's torso
mrq	radius of leader's quad
mrc	radius of leader's calf
mrb	radius of leader's bicep
mrf	radius of leader's forearm
frt	radius of follower's torso
frq	radius of follower's quad
frc	radius of follower's calf
frb	radius of follower's bicep
frf	radius of follower's forearm

Table 3.4: Notation for the radius of each body part as represented by a cylinder.

Body Mass Notation	
mmt	mass of leader's torso
mmq	mass of leader's quad
mmc	mass of leader's calf
mmb	mass of leader's bicep
mmf	mass of leader's forearm
fmt	mass of follower's torso
fmq	mass of follower's quad
fmc	mass of follower's calf
fmb	mass of follower's bicep
fmf	mass of follower's forearm

Table 3.5: Notation for the estimated mass of each body part based on the dancers overall mass.

3.7 Mass Notation

To fully define the bodies we also considered the mass of each body part. In order to estimate this mass we used a system developed by Nickolova to divide the total mass of the body into fractions of the total mass that existed in each body part [7]. Each dancer's total mass was self-reported by the dancers. Table 3.5 provides the notation used for the mass of each body part.

Chapter 4

Constraining the Model

In addition to defining the size parameters of each dancer and defining his pose, our model also had to consider the ways a person could actually move. For example, in an unconstrained model, each joint angle could take any value. If unconstrained, the joint representing the knee could be bent completely backwards, or the dancer might be in a limbo position where their back is parallel to the ground and their hips are thrust inward. Figures 4.1 and 4.2 represent examples of these unnatural poses.

If these pictures represented a machine that was simply looking for the most efficient spin position and that could balance and bend in any position then the poses illustrated by 4.1 would be fine. However, since our model is representing a human pose, the values of the angles in the pose must be constrained so that the dancer's position is biologically reasonable.

4.1 Pose Constraints

The first pose constraint we added was a restriction on the hips, so they could not thrust inward. Even though people can thrust their hips inward, we know from observing dancers and trying to pose in that way ourselves that it is not a pose from which one can easily begin to start spinning. The hip constraints are represented by the following equations added as constraints in the optimization:

$$\begin{aligned} \theta_{mh} + \theta_{mkg} &\leq \pi \\ \theta_{mh} + \theta_{mkp} &\leq \pi \\ \theta_{fh} + \theta_{fkg} &\leq \pi \\ \theta_{fh} + \theta_{fkp} &\leq \pi \end{aligned}$$

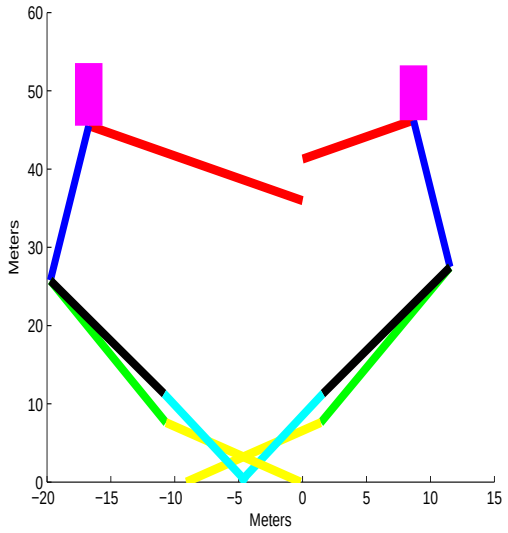

Figure 4.1: In this unconstrained model the dancers feet are crossed, their knees are bending the wrong direction, and they are not rotating around the correct axis.

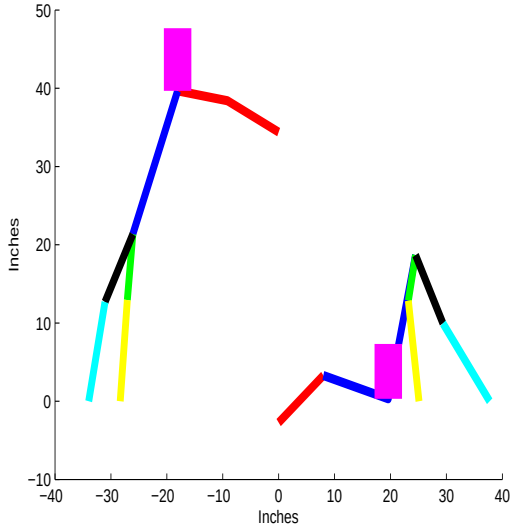

Figure 4.2: In this picture one of the dancers is entirely bent over so that his shoulders are on the floor and he is entirely disconnected from his partner.

Also, human knees have a limited range of motion. They cannot be bent backwards. As they are defined in our model, the angle at the feet($\theta ffg, \theta mfg$) must always be greater than ($\theta fkg, \theta mkg$) the angle of the knee. These constraints are represented by:

$$\begin{aligned} \theta_{mkp} - \theta_{mfp} &\leq 0 \\ \theta_{mkg} - \theta_{mfg} &\leq 0 \\ \theta_{fkp} - \theta_{ffp} &\leq 0 \\ \theta_{fkg} - \theta_{ffg} &\leq 0 \end{aligned}$$

The elbow is also limited in its range of motion. Since we are limiting the movement of the shoulder to the 2-dimensional yz-plane any pose with the elbow bent backward would require the elbow to be broken. The elbow constraint is represented much like the knee constraints except for its direction:

$$\begin{aligned} \theta_{mb} - \theta_{mf} &\geq 0 \\ \theta_{fb} - \theta_{ff} &\geq 0 \end{aligned}$$

The final constraint that is strictly a function of pose is a constraint on the value of the hip angle. Early in our optimization attempts we would occasionally get a value for the angle of the hip that was negative or near zero. Any angle at or below zero creates a pose where the dancer is entirely bent forward with her torso nearly level with the floor. While this pose might create a more minimal moment of inertia, we know that people cannot dance like this. The hip constraint is simply: $\theta_{mh} \geq \frac{\pi}{4}$ and $\theta_{fh} \geq \frac{\pi}{4}$. These values force the hip angle to maintain a pose that is biologically sound.

All of the above constraints ensure that the only allowable pose outputs from the optimization are biologically reasonable poses. We did not want to overly constrain our solution. The constraints listed above should only require that the dancer be in a pose that a human being could assume and spin in.

4.2 Tripping Constraint

In addition to the constraints required to make the pose humanly attainable, we also add restrictions on the ranges of the feet and each of the joints to the axis of rotation. An optimization scheme could determine the best pose would place a dancer's feet on the other side of the axis of rotation crossed over his partner's feet. See Figure 4 for an illustration of this pose. This pose might create a small moment of inertia,

however, it is a difficult position from which to begin rotating and not particularly stable (dancers might trip).

To eliminate this pose and any other poses where the dancers might be so close that their lower body ends up invading their partner's body space, we require that the distances to each dancer's joints defined in the model are positive:

$$\begin{aligned} mRfg \geq 0 \quad & fRfg \geq 0 \\ mRfp \geq 0 \quad & fRfp \geq 0 \\ mRkg \geq 0 \quad & fRkg \geq 0 \\ mRkp \geq 0 \quad & fRkp \geq 0 \\ mRh \geq 0 \quad & fRh \geq 0 \\ mRs \geq 0 \quad & fRs \geq 0 \\ mRE \geq 0 \quad & fRE \geq 0 \end{aligned}$$

4.2.1 Hand Constraint

The dancers were connected at the hands. Each of the two dancers had unique size parameters and could assume a different pose. The height of each dancer's hands was dependent on his or her pose. Therefore, we wrote a constraint requiring that the height of the dancers' hands be equal so that they could hold hands, $fHhand - mHhand = 0$.

4.3 Hip Height Constraint

The height of the hip was determined by the pose of the grind leg. However, the height of the hip is separately determined by the pose of the push leg. These two values must be equal, $fHh - fHhip = 0$. The fHh variable represents the location of the hip as defined by the grind foot and $fHhip$ represents the height of the hip as defined from the push foot. This constraint prevents the model from creating a disconnected dancer.

4.4 Grind Foot Location Constraint

As our model is defined, the dancers are pulling on their partner's hands creating a tension between them. We did not consider the potential that the dancers would

pose in such a way that they would be pushing on one another. Thus, in order to maintain their balance and not push on their partner the dancers grind feet must be in front of their respective center of mass:

$$fxCoM - fRfg \geq 0$$
$$-mxCoM - mRfg \geq 0$$

This constraint will not allow the optimizer to consider any pose that would require the dancers to be leaning into one another.

Chapter 5

Calculating and Optimizing Moments of Inertia

5.1 Inertia Calculation Methodology

We calculated the moment of inertia of the dance couple. That dancers minimize moment of inertia seemed plausible because an object's moment of inertia is its resistance to initiating a spin. The dancers might be able to spin faster by minimizing this initial resistance to spin.

We used a planar model to calculate the moment of inertia for a couple. We determined the mass for all parts of the body by partitioning a dancer's mass as described in Table 3.5 and by Niklova [7]. Lengths of different body parts are labeled with an L and a letter representing the part of the body that it is measuring. The lengths of each body part were determined for each couple based on video analysis. We calculated numerically the ideal fixed angles the dancers should choose to minimize the moment of inertia. These angles were designated in much the same way as the lengths and were measured as related to the horizontal. For a full listing of the length and angle parameters refer to tables 3.3 and 3.1.

This model was first applied to one dimensional thin rods and then expanded to non-right cylinders. We do not elaborate here on the calculations of moment of inertia for one-dimensional rods. Some optimization results for this model are shown in section 5.2. The first step in calculating moment of inertia was completed as a part of the modeling process, which was to define distance to the axis of rotation for each component of the body. This process was explained in the previous chapter and all the variable names are listed in Table 3.3. Once these distances are determined we

apply the parallel axis theorem.

5.1.1 Parallel Axis Theorem

We calculated the moment of inertia of each body segment in a given pose by twice applying the parallel axis theorem. The parallel axis theorem allows us to find the moment of inertia of a body rotating around an axis by providing a mechanism for calculating the moment of inertia around the center of mass of that body and then shifting the object over a specified amount. The parallel axis theorem states:

$$I_{new} = I_{com} + Md^2$$

where I_{new} is the moment of inertia of the body rotating around an axis at some distance, d, from its center of mass, I_{com} is the moment of inertia of the object around its center of mass, and M is the mass of the object.

In our model, the dancer's body was defined as a collection of possibly non-right cylinders. To find the moment of inertia of the dancer, we find the moment of inertia of each part of the body and then sum the individual moments of inertia. To find the moment of inertia of a single body part modeled as a non-right cylinder we applied the parallel axis theorem as an integral over the length of the cylinder.

5.1.2 Integrals over non-right cylinders

Integrals were used because integrals can represent a sum of infinitely thin objects stacked on top of one another. Using the moment of inertia of a thin disk, $I_{disk} = \frac{1}{2} * M * R^2_{disk}$, and then taking the integral over the length of the non-right cylinder to sum the moments of inertia of the individual disks, we can calculate the moment of inertia of the cylinder rotating around its center of mass.

Figure 5.1 shows an example of a non-right cylinder and labels how all of the variables in the integration would be labeled. The radius of the cylinder is labeled $r_{cylinder}$ and is also the radius of the thin disk. The distance that each disk would be offset from the center of mass of the cylinder is labeled r and R is the distance from the center of mass of the cylinder to the axis the dancer is rotating around. The calculations for the moment of inertia of a single body part are illustrated below. We begin by calculating the moment of inertia of a single thin disk:

$$I_{disk} = \frac{1}{2} * R^2_{cylinder} + Mr^2$$

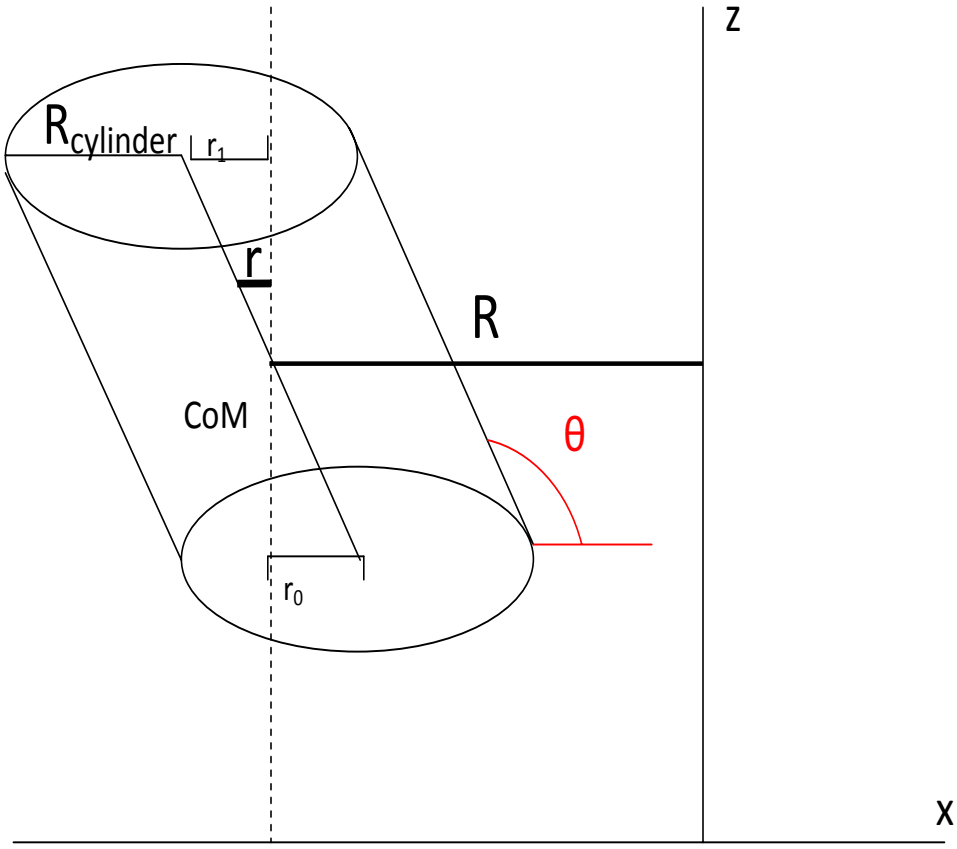

Figure 5.1: A model of the cylinder that defines the different variables used in the integration for the moment of inertia.

Integrating over the length of the cylinder sums the moments of inertia of the individual disks and determines the moment of inertia of the whole cylinder. We also use the parallel axis theorem again by adding an additional Md^2 term that will account for the shift of the cylinder from rotating around its own center of mass to rotating around a center of mass some distance away. The new inertia would be represented as:

$$I_{segment} = \int_{r_o}^{r_1} I_{disk} dr + MR^2$$

Combining the two equations listed above, we calculate the moment of inertia of the body segment rotating around the axis of rotation of the dancer's spin as:

$$I_{segment} = \int_{r_o}^{r_1} (\frac{1}{2} * R_{cylinder}^2 + Mr^2)_{r_o}^{r_1} dr + MR^2$$

As an example of the above calculation we can look at the results for one of the body parts. The above calculations result in an equation for the moment of inertia of the torso of:

$$\begin{aligned} &fInertiaTorso = \\ &\quad \frac{1}{2} fmt * frt^2 + \\ &\quad \frac{1}{12} * fLt^2 * fmt * Cos[\theta fh]^2 * Sin * [\theta fh] + \\ &\quad fmt * (fRs + \frac{1}{2} * fRh)^2 \end{aligned}$$

where $\frac{1}{2} fmt * frt^2$ is the inertia for a single thin disk around its center of mass. The $\frac{1}{12} * fLt^2 * fmt * Cos[\theta fh]^2 * Sin * [\theta fh]$ is the result of the integral that sums all of the disks over the length of the cylinder. Finally the $fmt * (fRs + \frac{1}{2} * fRh)^2$ term equates to the MR^2 term above and shifts the entire moment of inertia from rotating around its own center to rotating around the axis some distance away. The length, distance and angle variables are defined in Tables 3.1, 3.3, and 3.3.

5.1.3 Limitations and Putting it all Together

To simplify the calculations, the hands and feet were taken as extensions of the arms and legs instead of as separate bodies. We neglected the contribution of the hands and feet to the moment of inertia. The model also does not allow for motion in the neck and constrains the motion of the hip, legs, and arms to planar motion in the

xz-plane. We treat all joints as hinge joints with only one degree of freedom. When the moment of inertia of each piece of the body including the arms, head, torso, and each leg is calculated, the moments are summed together to obtain the moment of inertia for the dancer.

5.2 Optimizing the Moment of Inertia

5.2.1 Minimizing the Simple Stick Model

Our original model had only a foot angle, and then we added a hip angle. We rejected this model because the solutions it gave us were not representative of what we saw dancers actually doing. When we minimized the moment of inertia with only a foot angle the answer ended up at our foot crossing constraint. This result held that the optimal position would be for the dancers to put both feet right at the axis of rotation. This answer is not physically realistic because from that point they have no ability to produce force to begin spinning. Also, as illustrated by Figure 5.2, the optimal solution exists right at the boundary we set. Since the optimal solution lands right at one of the constraints, we know that the solution is artificially bounded by one of our constraints. The model that minimizes moment of inertia is not rich enough to capture some essential aspects of the partnered spin.

5.2.2 Further Minimization with Hip Angle

We added an angle at the hip to add more flexibility to the problem. However, minimizing the moment of inertia yielded the same pose as we had with the simpler model. We postulated that any further complexity in the form of joint angles added to this model would be meaningless because they would continue to come back to this position. Additionally, in a similar way as to the single angle problem, the optimal solution butted up against the constraints we set on the problem. Figure 5.3 illustrates the unconstrained pose and the optimal solution corresponds with the red star on Figure 5.6. We added the hip constraint from Section 4.1. With this constraint we got the pose represented in Figure 5.4 whose corresponding optimal solution is represented by the yellow star on Figure 5.6. For Figure 5.5 we added the foot crossing constraint (Section 4.2) in addition to the hip constraint. This pose illustrated in Figure 5.5 corresponds to the green star on Figure 5.6. This work convinced us that minimizing moment of inertia would not produce an output that would convincingly represent the pose for a partnered spin. When we moved on to

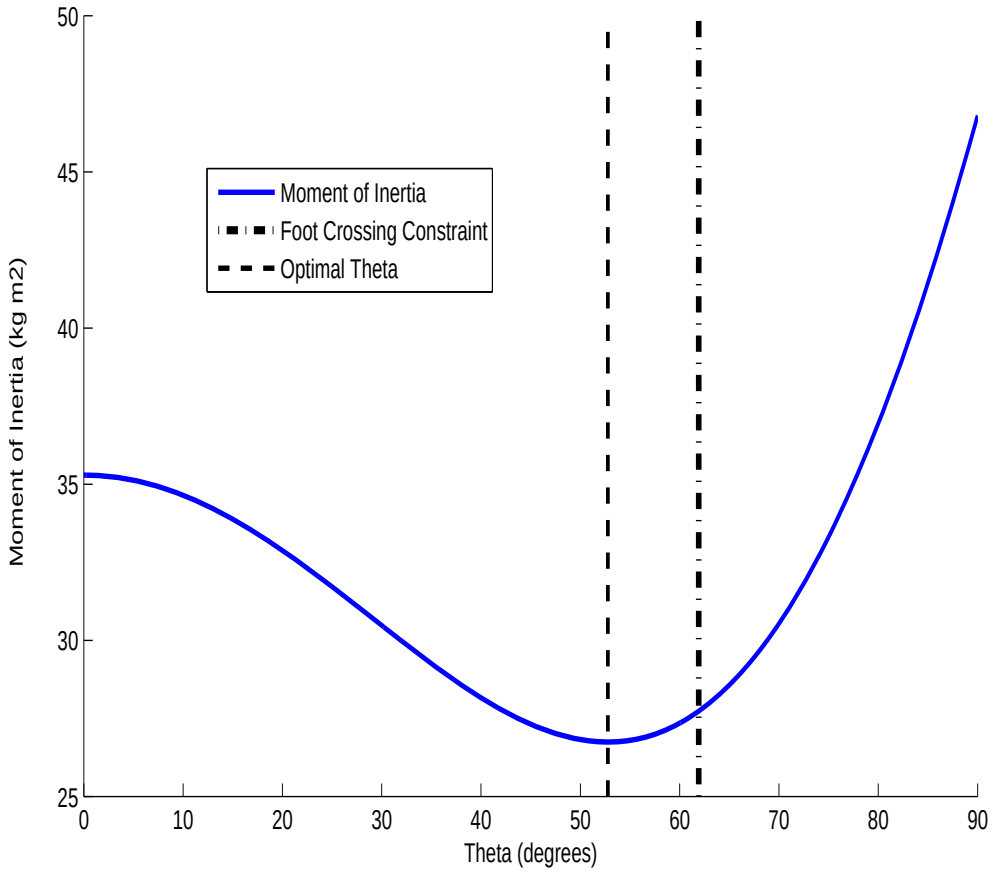

Figure 5.2: The graph that was produced for the optimization of the dancer with only one angle.

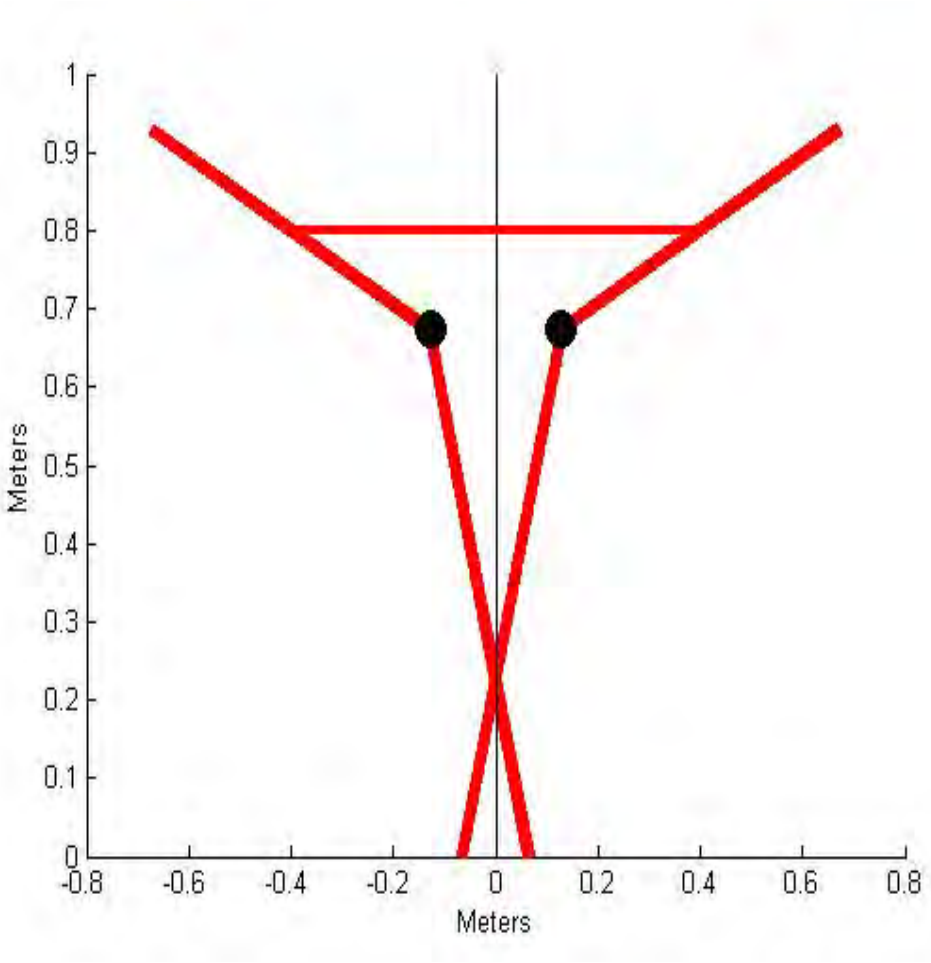

Figure 5.3: The unconstrained optimal pose.

our more advanced model based on maximizing the angular acceleration all of our moment of inertia work was put into use as a piece of that model.

Minimizing the moment of inertia is not a rich enough problem. The answer aligned to the constraints we set on what the person could physically do. To minimize their moment of inertia, the dancers should stand up straight and get very close together. This position does not allow for the dancers to produce any torque to spin. They need one of their feet to have some distance from the axis in order to have a moment arm to apply a rotational force and create torque. We know dancers do not dance with both feet right at the axis and thus we determined that minimizing moment of inertia was not sufficient for understanding why dancers adopt the poses they do.

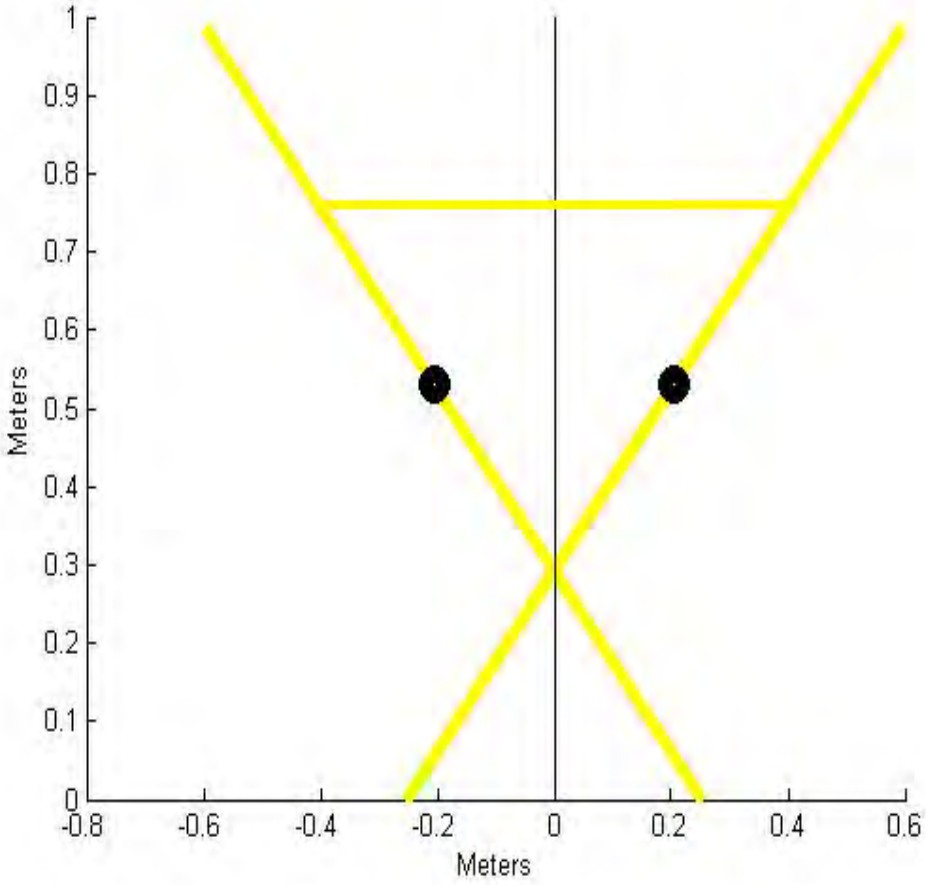

Figure 5.4: The optimal pose with the hip constraint.

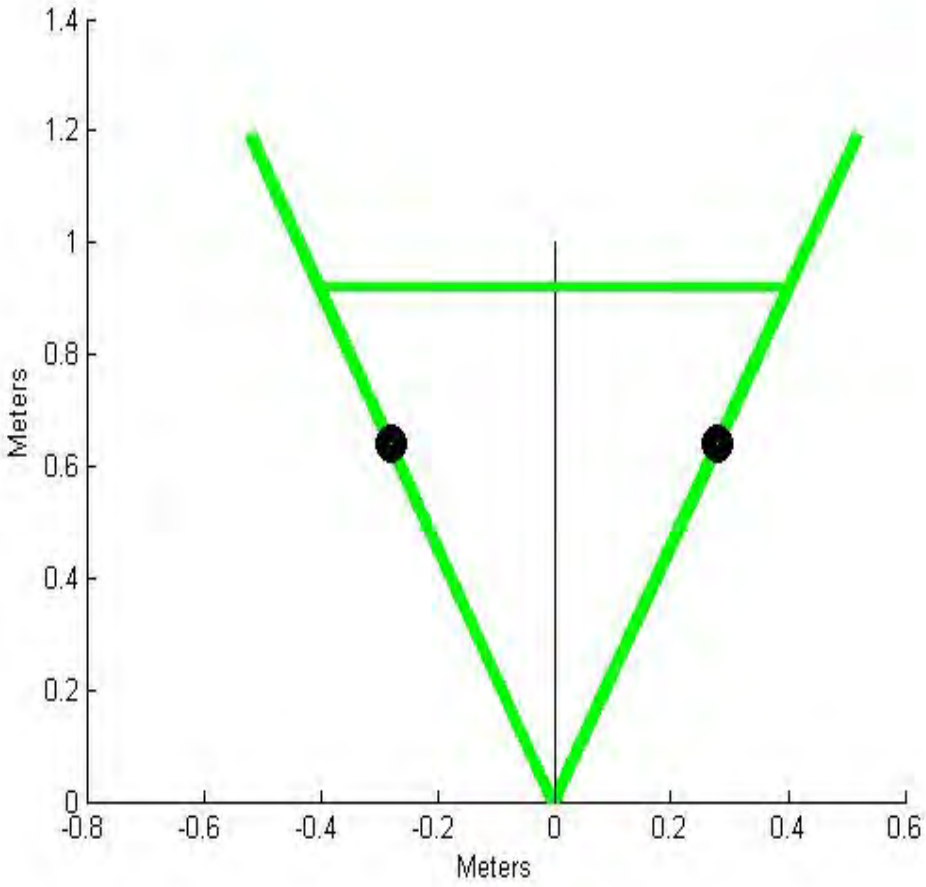

Figure 5.5: The fully constrained optimal pose.

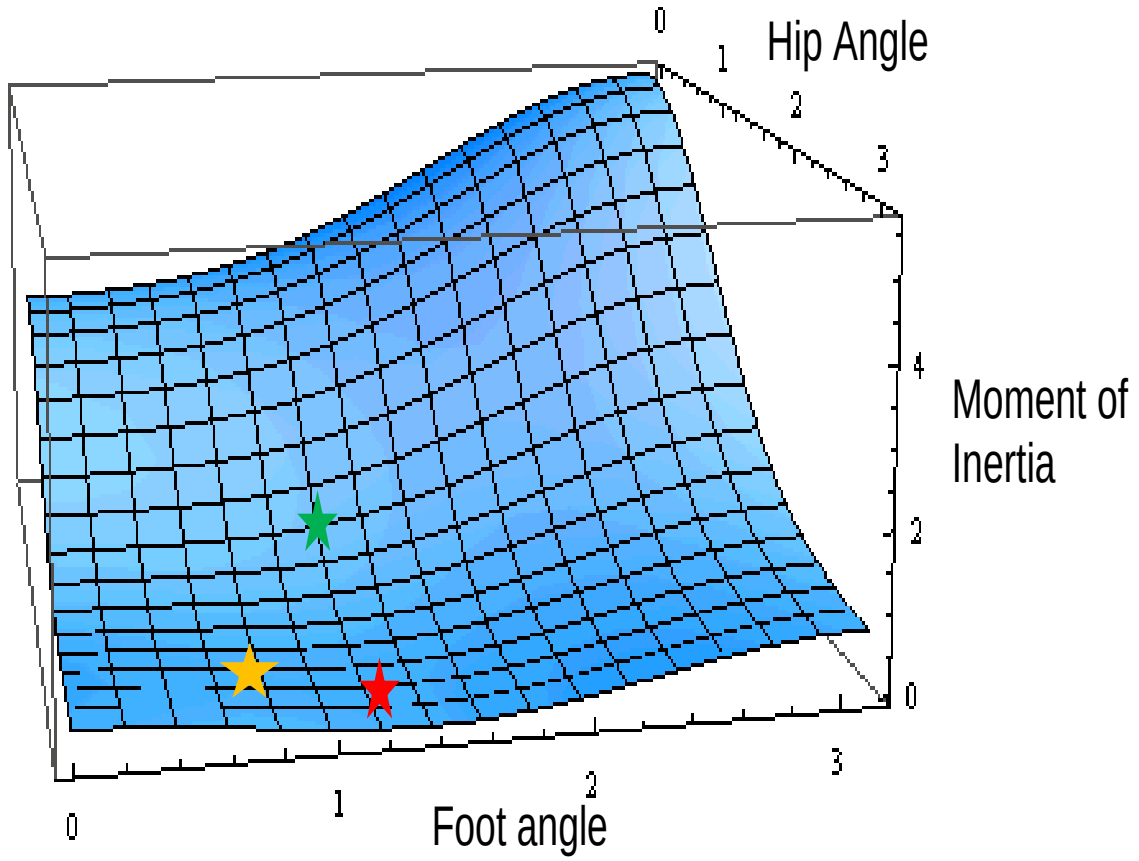

Figure 5.6: This graph illustrates the value of the moment of inertia for each of the previous three poses. The red star corresponds with the unconstrained solution (Figure 5.3) and has the lowest moment of inertia. The yellow star corresponds with the solution with the hip constraint (Figure 5.4) and has a slightly higher moment of inertia. The green star corresponds with the fully constrained solution (Figure 5.5) and has the highest moment of inertia.

Chapter 6

Calculating and Maximizing Angular Acceleration

6.1 Angular Acceleration Models

In modeling the spinning motion of dancers, we use their size parameters to determine the best pose for a couple by maximizing their angular acceleration. This model appears to output realistic poses for the Lindy Hop rhythm circle. The ideal pose is deemed to be a pose that maximizes the angular acceleration of the dancers. The angular acceleration, $\alpha[\Theta]$, is calculated as:

$$\begin{aligned} \alpha[\Theta] &= \frac{\tau[\Theta]}{I[\Theta]} \\ \Theta &= [\theta_{ff}, \theta_{fb}, \theta_{fh}, \theta_{fkg}, \theta_{fkp}, \theta_{ffg}, \theta_{ffp}, \theta_{mf}, \theta_{mb}, \theta_{mh}, \theta_{mkg}, \theta_{mkp}, \theta_{mfg}, \theta_{mfp}] \end{aligned}$$

where tau,$\tau[\Theta]$, is the torque produced by the dancer as a function of Θ and the moment of inertia, $I[\Theta]$, is the dancers' resistance to initiating a spin. Theta, Θ, is a vector of angles that define both dancers' poses. All angles are calculated with relation to the horizon as illustrated in Figure 3.4.

We should clarify that $\tau[\Theta]$ is not taken from experimental data, but is calculated instead. Calculating the correct Tau, $\tau[\Theta]$, was one of the most challenging parts of building the model. The first step in determining $\alpha[\Theta]$ is to determine the moment of inertia.

6.2 Accounting for Forces

Our first objective function neglected the need to produce torque in order to spin, so we decided to maximize angular acceleration instead. Angular acceleration, $\alpha[\Theta]$, is equal to $\frac{\tau[\Theta]}{I[\Theta]}$. This objective incorporates the dancers' ability to create torque from a given pose while minimizing the moment of inertia.

Torque, τ, is the force which causes an object to spin and produces angular acceleration. Tau can not be arbitrarily large because the force is generated by the dancer pushing against the floor, and there is a limit beyond which the dancer's foot will slip. All of the external forces acting on the dancers are related to one another. Figure 6.1 illustrates all of these forces acting on the dancers. There are in fact only four independent forces at work as the dancer spins: the force of gravity acting through the center of mass, the force acting at her hands from her partner pulling on her, and the force from the floor acting on each of her two feet. The feet are distinguished as the push foot and the grind foot

In Figure 6.1 each of these forces is broken down into components in the x,y, and z axes. In order to sufficiently constrain our problem we had to set the force acting at the hands in the y and z axes to be zero. Thus the force at the hands is only represented by a single arrow in this picture. Additionally because gravity only acts in the z direction it was also only represented with a single arrow. The forces on each of the feet were separated into their x,y,z components.

The known force of *gravity* acts through the center of mass of the dancer in the z-direction and is equal to $9.8\frac{m}{s^2} * fMass$. $fFxHands$ is the force in the x-direction on the follower from her partner pulling on her hands while $mFxHands$ is the equivalent force on the leader from the follower pulling on his hands. While $fFyHands$, $fFzHands$, $mFyHands$, and $mFyHands$ do exist, they are not illustrated because for the purposes of our model we set them equal to zero. $fFgrindVert$ is the force in the x-direction on the follower's grind foot that is a result of friction and represents her tendency to slide toward or away from her partner. $mFgrindVert$ represents the equivalent force to $fFgrindVert$ for the leader. $fFpushVert$ is the force in the x-direction on the follower's push foot. $mFpushVert$ represents the force in the x-direction acting on the leader's push foot. $fFgrindHort$ and $fFpushHort$ are the forces acting on each of the follower's feet in the z-direction. These forces are often referred to as normal forces. $mFgrindHort$ and $mFpushHort$ are the normal forces on the leader's feet.

Finally $fFpushSpin$ is the force on the follower's push foot in the y-direction that will induce motion that will initiate the spin. These forces are the most crucial forces in our model because they are the forces that induce the spin. Our goal was to find

xCoM calculations and zCoM calculations	
$fxCoMf = fRe/2 * fmf$	$fzCoMf = (fHE + fHh)/2 * fmf$
$fxCoMb = (fRs + fRe)/2 * fmb$	$fzCoMb = (fHs + fHE)/2 * fmb$
$fxCoMt = (fRs + fRh)/2 * fmt$	$fzCoMt = (fHs + fHh)/2 * fmt$
$fxCoMqg = (fRkg + fRh)/2 * fmqg$	$fzCoMqg = (fHh + fHkg)/2 * fmqg$
$fxCoMqp = (fRkp + fRh)/2 * fmqp$	$fzCoMqp = (fHh + fHkp)/2 * fmqp$
$fxCoMcg = (fRkg + fRfg)/2 * fmcg$	$fzCoMcg = fHkg/2 * fmcg$
$fxCoMcp = (fRkp + fRfp)/2 * fmcp$	$fzCoMcp = fHkp/2 * fmcp$
$mxCoMf = mRe/2 * mmf$	$mzCoMf = (mHE + mHh)/2 * mmf$
$mxCoMb = (mRs + mRe)/2 * mmb$	$mzCoMb = (mHs + mHE)/2 * mmb$
$mxCoMt = (mRs + mRh)/2 * mmt$	$mzCoMt = (mHs + mHh)/2 * mmt$
$mxCoMqg = (mRkg + mRh)/2 * mmqg$	$mzCoMqg = (mHh + mHkg)/2 * mmqg$
$mxCoMqp = (mRkp + mRh)/2 * mmqp$	$mzCoMqp = (mHh + mHkp)/2 * mmqp$
$mxCoMcg = (mRkg + mRfg)/2 * mmcg$	$mzCoMcg = mHkg/2 * mmcg$
$mxCoMcp = (mRkp + mRfp)/2 * mmcp$	$mzCoMcp = mHkp/2 * mmcp$

Table 6.1: Calculations for the x-coordinate of the center of mass, $xCoM$, and z-coordinate for the center of mass, $zCoM$, for the follower and leader.

a method for estimating these forces. This force is countered by $fFgrindspin$ which is the force in the y-direction at the grind foot. $mFpushSpin$ and $mFgrindSpin$ are the leader equivalents for these two forces.

While there are only 8 external forces controlling this system, calculating these forces is a challenging problem. One of the first steps in solving it is to determine the location of the center of mass for a dancer in a given pose [13].

6.2.1 Finding the Center of Mass

Gravity acts through an object's center of mass. We used our segmented body model to calculate the center of mass, and we calculated the x, y, and z components of the center of mass separately. The center of mass of each body segment is the average of the two end points of a body part.

For example, the x-coordinate of the center of the torso is $xCoMt = (Rs + Rh)/2$. A weighted average of these values determined x-coordinates of the center of mass of the body. Similar calculations yield the location of the z-coordinate of the center of mass. Because our model did not allow for any movement in the y-axis, we set the y-coordinate of the center of mass to zero.

To determine the weight of each body part we used work by Nikolova and Toshev on the population of Bulgaria [7]. They developed a standard for the percentage of a person's weight that is in each of his or her body parts. While this method will not provide a precise distribution for each individual, it allows us to easily estimate the distribution for all of the subjects. The calculations for the center of mass are in Table 6.1.

6.3 Dynamic Model

To find the six unknown forces we defined earlier, we considered them as a part of the whole system that defined the movements of the dancers. Our model has 27 degrees of freedom. Three forces $FHands$, $FPush$, $FGrind$ for each of the two people (leader and follower) creates the six unknown forces mentioned earlier (Figure 6.1). These forces potentially act in three dimensions (x,y,z), for 18 degrees of freedom. Let α represent the angular acceleration of the dancers, ω represent the angular velocity of and let a represent the linear acceleration of the dancers. The dynamic elements of α, ω, and acceleration, a, in three dimensions (x,y,z) account for the other 9 degrees of freedom. These terms accounted for the movements of the dancers. While this system has many degrees of freedom, it is also highly constrained. First, the system is constrained by two vector equations from Newton's 3rd law:

$$\sum F_i = M * a \tag{6.1}$$

$$\sum \tau_i = I\alpha = \sum r_i \times F_i \tag{6.2}$$

Equation 6.1 states that the sum of the various forces acting on an object, indexed by the variable i, is equal to the product of the mass of the object and its linear acceleration. Equation 6.2 is the rotational equivalent of equation 6.1 stating that the sum of the torques is equal to the product of the moment of inertia of the object and its angular acceleration. Each torque, τ_i, is the cross product of r_i, the distance from the axis of rotation to the point of application of the force, and F_i, the force acting at that distance.

These two definitions from Newton's law account for six equations per dancer:

$$fInertiaTotal * \alpha_f = \sum r_i \times F_i \tag{6.3}$$

$$fMass * a_f = \sum F_i \tag{6.4}$$

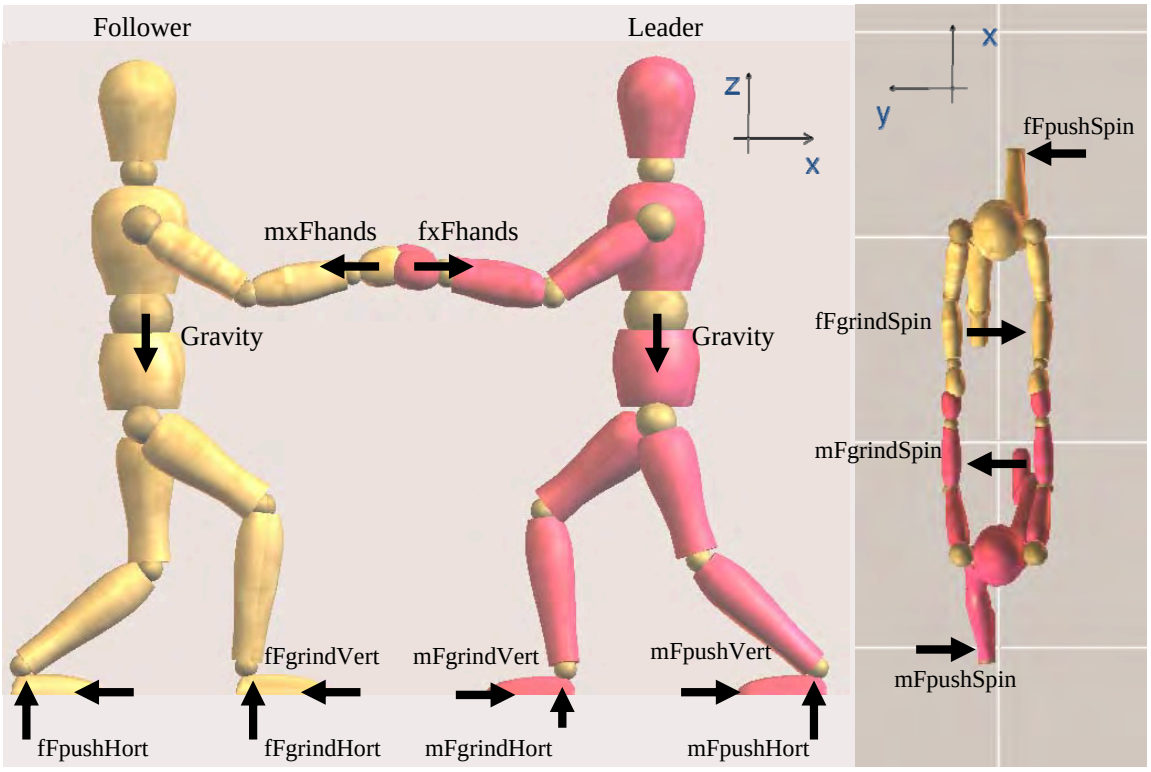

Figure 6.1: All of the forces acting on the system to cause it to rotate.

Both equations 6.3 and 6.4 are vector equations that translate into 3 scalar equations each. These equations also apply to the leader:

$$mInertiaTotal * \alpha_m = \sum r_i \times F_i \quad (6.5)$$

$$mMass * a_m = \sum F_i \quad (6.6)$$

Equations 6.4 and 6.6 give six scalar equations. Sum of the forces in the x-axis:

$$fMass * fxCoM * \omega_{fz}^2 = fFxHands + fFgrindHort + fFpushHort \quad (6.7)$$

$$mMass * mxCoM * \omega_{mz}^2 = mFxHands + mFgrindHort + mFpushHort \quad (6.8)$$

These two equations listed above our extremely important because they show that the force at the hands between the dancers is responsible for their rotational motion. Except in certain unique poses, $fFgrindHort + fFgrindPush = 0$, which leaves $fFxHands$ equal to the rotational motion of the dancers. Next, the sum of the forces in the y-axis:

$$0 = fMass * fxCoM * \alpha_{fz} - fFpushSpin + fFgrindSpin \quad (6.9)$$

$$0 = -mMass * mxCoM * \alpha_{mz} + mFpushSpin - mFgrindSpin \quad (6.10)$$

These equations show the forces that initiate the movement by pushing off the floor. Finally the sum of the forces in the z-axis:

$$fFgrindVert + fFpushVert = fMass * gravity \quad (6.11)$$

$$mFpushVert + mFgrindVert = mMass * gravity \quad (6.12)$$

These two equations simply illustrate that gravity is present and working on the system.

Using 6.3 and 6.5 the angular equivalent of Newton's 3rd law, gives six more equations. The sum of the moments around the x-axis:

$$0 = fFxHands * fHhand - fFgrindVert * fRfg - fFpushVert * fRfp + fMass * fxCoM * gravity \quad (6.13)$$

$$0 = mFxHands * mHhand - mFgrindVert * mRfg - mFpushVert * mRfp + gravity * mMass * mxCoM \quad (6.14)$$

These equations show that we are not tipping over forward or back. Summing the moments of inertia around the y-axis gives:

$$0 = fFgrindVert * frt + fFpushVert * frt \quad (6.15)$$

$$0 = mFgrindVert * mrt + mFpushVert * mrt \quad (6.16)$$

The moments around the x and y axes were equal to zero because the dancers were not rotating in those axes. The two equations above illustrate that the dancers are not falling over to the side. The moments in the z-axis are equal to the product of moment of inertia and the angular acceleration. These equations are critical because this is the rotation we focused on and the one we were trying to maximize. The sum of the moments around the z-axis are:

$$\begin{aligned} \alpha_{fz} * fInertia &= fFgrindSpin * fRfg + fFpushSpin * fRfp - \\ &\quad fFgrindHort * fyfg - fFpushHort * fyfp \qquad (6.17) \\ \alpha_{mz} * mInertia &= mFgrindSpin * mRfg + mFpushSpin * mRfp - \\ &\quad mFgrindHort * myfg - mFpushHort * myfp \qquad (6.18) \end{aligned}$$

The above equations were all derived from Newton's 3rd law and account for 12 constraints on the system.

Restrictions on α and ω further constrain the system. In our problem, the dancers were only spinning around the z-axis. Thus the angular acceleration and angular velocity in the other two axes are equal to zero:

$$\alpha_{mx} = \alpha_{fx} = 0 \qquad (6.19)$$
$$\omega_{mx} = \omega_{fx} = 0 \qquad (6.20)$$

$$\alpha_{my} = \alpha_{fy} = 0 \qquad (6.21)$$
$$\omega_{my} = \omega_{fy} = 0 \qquad (6.22)$$

In the z-direction the angular acceleration and angular velocity are constrained by the fact that the two dancers are moving as a single unit. The dancers must have the same angular acceleration and angular velocity:

$$\alpha_{mz} = \alpha_{fz} = \alpha_{couple} \qquad (6.23)$$
$$\omega_{mz} = \omega_{fz} = \omega_{couple} \qquad (6.24)$$

These restrictions on the angular accelerations and angular velocities of the dancers provide an additional 6 constraints on the system for a tally of 18. Because the dancers are rotating and not traveling in any direction, a constraint can be placed on the magnitude of the linear acceleration a. In this problem, the dancers as a unit are not accelerating linearly:

$$a_x = 0 \qquad (6.25)$$
$$a_y = 0 \qquad (6.26)$$
$$a_z = 0 \qquad (6.27)$$

This restriction brings our number of constraints up to a total of 21. Newton's 2nd law states that for every force there is an equal and opposite reaction force. The force at the hands must be equal and opposite between the two dancers:

$$fFxHands = mFxHands \tag{6.28}$$

This removes another degree of freedom. It also reminds us that the force at the hands has already been constrained because we have defined its value in the y and z axes to be zero:

$$0 = fFyHands = mFyHands \tag{6.29}$$
$$0 = fFzHands = mFzHands \tag{6.30}$$

With all of the constraints listed above, our system includes 24 constraints. We also assumed that the dancers were pushing as hard as they could against the floor without slipping. This assumption gives two equations:

$$(mFpushVert * \mu s)^2 = (mFpushHort^2 + mFpushSpin^2) \tag{6.31}$$
$$(fFpushVert * \mu s)^2 = (fFpushHort^2 + fFpushSpin^2) \tag{6.32}$$

With this system of equations we attempted to solve for 16 unknowns. We planned to determine the force in all three directions on each of the feet, the force at the hands in the x-axis, and the angular acceleration, α, around the z-axis. This system could not be solved analytically. We used Mathematica to solve our large systems of equations, and was unable to generate a solution to this system. We assume there must be a contradiction somewhere in the definition of the system, but we have been unable to locate it.

When we failed in solving this system, we also tried a different technique to use the same information to address our problem. We tried to use all of the equations as constraints in a maximization of the angular acceleration, α_z. This method also failed to net a satisfactory solution. With the high dimensionality of the problem and the extreme number of constraints imposed by that method, our optimization solver was unable to find any solutions that satisfied all of our constraints.

6.4 Final Model

While we were unable to garner a satisfactory solution from any of our previous attempts, we still wanted to find some method for interpreting the motion capture data that we had collected. Specifically, we wanted to distinguish between beginner and

expert dancers by comparing their performances according to a physically meaningful criterion. Chapters 8 and 9 will show that although we did not garner statistically significant results, the poses output from the model appear to be intuitively logical.

We used a simpler model that neglected $Fhands$, forces on the grind foot, and used a surrogate, $NormalPush$ for $FpushSpin$ which we could not calculate. We assume that the reaction forces from the floor are equal to the weight of the person over their push foot, which we estimate using the location of their center of mass. The biggest challenge in developing this model was accounting for the fact that the feet would not be in line, but would have some distance between them in the y-direction. This fact meant that we would calculate the distance from the axis of rotation to the location of the feet using Pythagorean theorem. The calculations for these distances for the follower (f) and the leader (m) were:

$$fDistPush = \sqrt{(fxCoM - fRfp)^2 + frt^2} \tag{6.33}$$

$$fDistGrind = \sqrt{(fxCoM - fRfg)^2 + frt^2} \tag{6.34}$$

$$mDistPush = \sqrt{(mxCoM - mRfp)^2 + mrt^2} \tag{6.35}$$

$$mDistGrind = \sqrt{(mxCoM - mRfg)^2 + mrt^2} \tag{6.36}$$

The variables used above were defined in Tables 3.3, 3.4, and 6.1. Using these distances we estimated what fraction of their weight was supported by their push foot:

$$fWeightPush = \frac{fDistGrind}{fDistGrind + fDistPush} \tag{6.37}$$

$$mWeightPush = \frac{mDistGrind}{mDistGrind + mDistPush} \tag{6.38}$$

The above fraction shows that if the dancer is standing mostly over her push foot than the distance between her center of mass and grind foot will be large. By the equation above then, this larger distance will equate to a larger fraction of her weight being over her push foot. Conversely, if $fDistGrind$ is small than most of the dancer's weight is over her grind foot not her push foot thus a small value for $fDistGrind$ corresponds to a smaller value for $fWeightPush$. By taking the product of the fraction of their weight over their push foot and their weight, we determined the normal force acting on the dancer's foot (see Section 6.2):

$$fNormalPush = fWeightPush * fMass * gravity \tag{6.39}$$

$$mNormalPush = mWeightPush * mMass * gravity \tag{6.40}$$

Using these normal forces, the simplifying assumption that the dancer would not push with any force in the x-direction and a an estimation of μs, the coefficient of static

friction, we made the claim that the normal force on the push foot is proportional to $fFpushSpin$. With this assumption we can calculate the push force to be:

$$fForcePush = fRfp * fNormalPush * \mu s \quad (6.41)$$

$$mForcePush = mRfp * mNormalPush * \mu s \quad (6.42)$$

Since both the leader and follower contribute to the force that causes the couple to spin, we sum these forces and divide by $InertiaTotal$ to estimate the angular acceleration:

$$\alpha = \frac{fForcePush + mForcePush}{InertiaTotal} \quad (6.43)$$

Even in this simple form, the model still contained 14 degrees of freedom. This simple model performed surprisingly well, giving us reasonable outputs for α in both the actual pose and the optimal pose, as well as plausible optimal poses. Figure 6.2 for an illustration of the model explained and refer to Chapter 9 for images of the actual and optimal poses, and values for α.

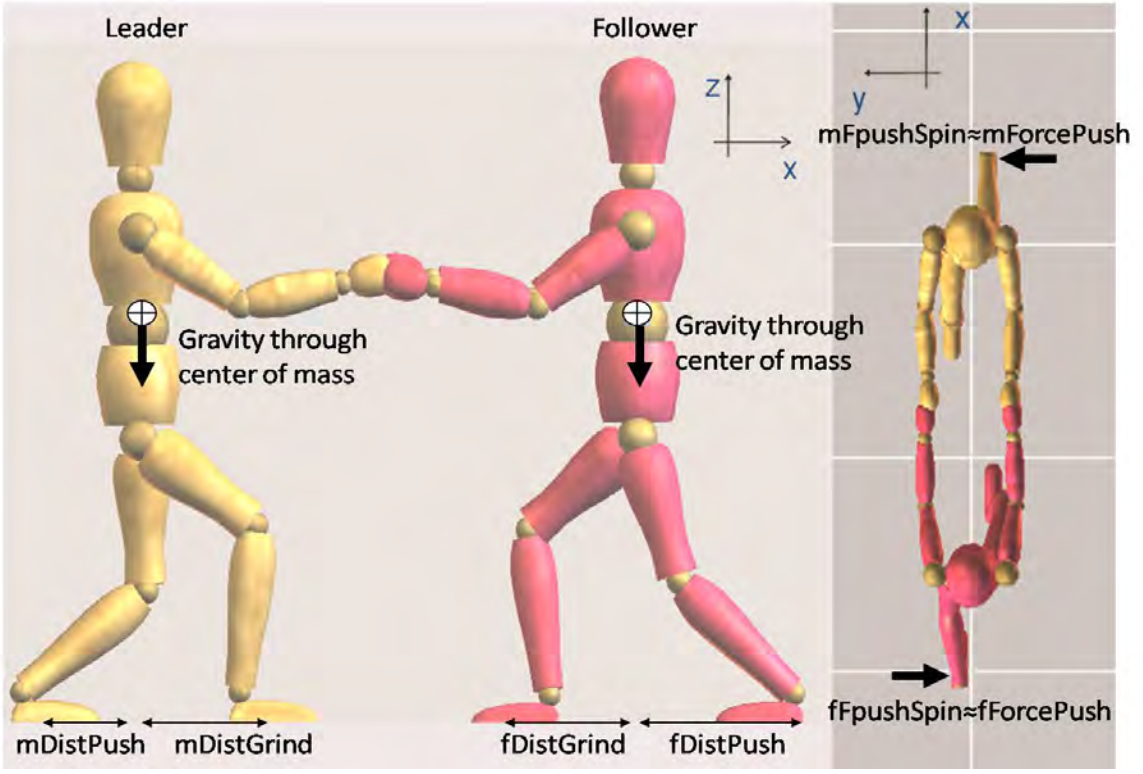

Figure 6.2: This figure illustrates the calculations for the surrogate model.

Chapter 7

Numerical Optimization

One challenging aspect of this project is optimizing the function estimating the angular acceleration of the dancers. We used the "NMaximize" function in Mathematica as our numerical optimization algorithm. Originally we planned to use analytical optimization to find a constrained function to represent the optimal pose, however, we quickly discovered that our system was too complicated to determine an analytic solution. For each couple we input individual size length and mass parameters to determine that couple's optimal and achieved accelerations. We solved a separate optimization problem for each couple.

Unfortunately, because Mathematica owns the rights to the "NMaximize" function we were not able to find details about how it works. Our "NMaximize" call maximizes α, the rotational acceleration estimate for the couple, subject to biological feasibility constraints on the pose. For a list of constraints see Chapter 4. The decision variables are the fourteen pose angles.

As we used "NMaximize", we became aware of a number its limitations. One of those is its sensitivity to the starting pose used for the optimization. The starting pose is a range of values from which the algorithm starts searching for an optimum. The optimizer may get stuck in a local optimum near the starting solution. We focused the pose for the optimization around the pose the couple actually held. While the optimal pose is very different from the initial pose, we discovered that the value of the objective at optimal varied even with slight changes in the initial pose.

We desired to determine the global maximum for the angular acceleration. The global maximum is the highest angular acceleration of any pose that fits the constraints and parameters of the problem. Determining the global optimum is much more difficult then determining a local optimum, which would just be the nearest

peak or valley in the solution. One method that could be employed to avoid getting stuck in local optima uses a combination of random start points and local optimization techniques to find the global optimum [10]. We found that there were times in our optimization that we did not reach a global optimum, but instead got stuck in a local optimum. One evidence of this fact is the variance in the "optimal" solution as described in the previous paragraph.

Another aspect of this problem that makes it particularly challenging is the high dimensionality. Figures 5.2 and 5.6 illustrate the optimal solutions to simple versions of our problem with only one and two decision variables, respectively. In its final form our model has 14 decision variables. Additionally, the function being optimized in both those figures is moment of inertia, which is relatively simple when compared to angular acceleration. Our problem has too many degrees of freedom for us to graph it, but we expect it to have many peaks and valleys as it is a non-convex function. This complexity combined with the high dimensionality of the problem makes it easy to get stuck in the local optima as mentioned above. We found that the "NMaximize" function was very sensitive to the starting locations that we put into it.

Chapter 8

Data Collection

8.1 Human Subject Research Approval

Before conducting any work involving human subjects, proper human subjects research approval was obtained from the US Naval Academy HRPP office.

8.2 Motion Capture System

Our motion capture system is a MaxTraq 3-D system developed by Innovision Systems. It consists of four video cameras that track highly reflective markers. When the four cameras are set up, a marked structure with known distances between the markers is placed in the field of view of all of the cameras and then recorded. This structure has six points, four on the floor and two in the air on a cross bar supported by legs on the structure. Figure 8.1 gives an illustration of this structure. This structure allows the system to calculate the position of each of the cameras so that it can develop accurate distances and velocities based on the motions it records. The calibration is very sensitive and even if the measurements of the structure our off by a small amount the system will not calibrate. We faced this challenge when six couples worth of data was unusable because of problems with the calibration.

This system can capture up to 100 points in one recording. We did not require 100 points, but this capability allowed us to easily capture the 19 points per a couple that we needed. Additionally, the system is designed so that a researcher can track subject manually by clicking on points every frame or make use of its auto-tracking feature which follows a point by looking for contrast between that point and the background

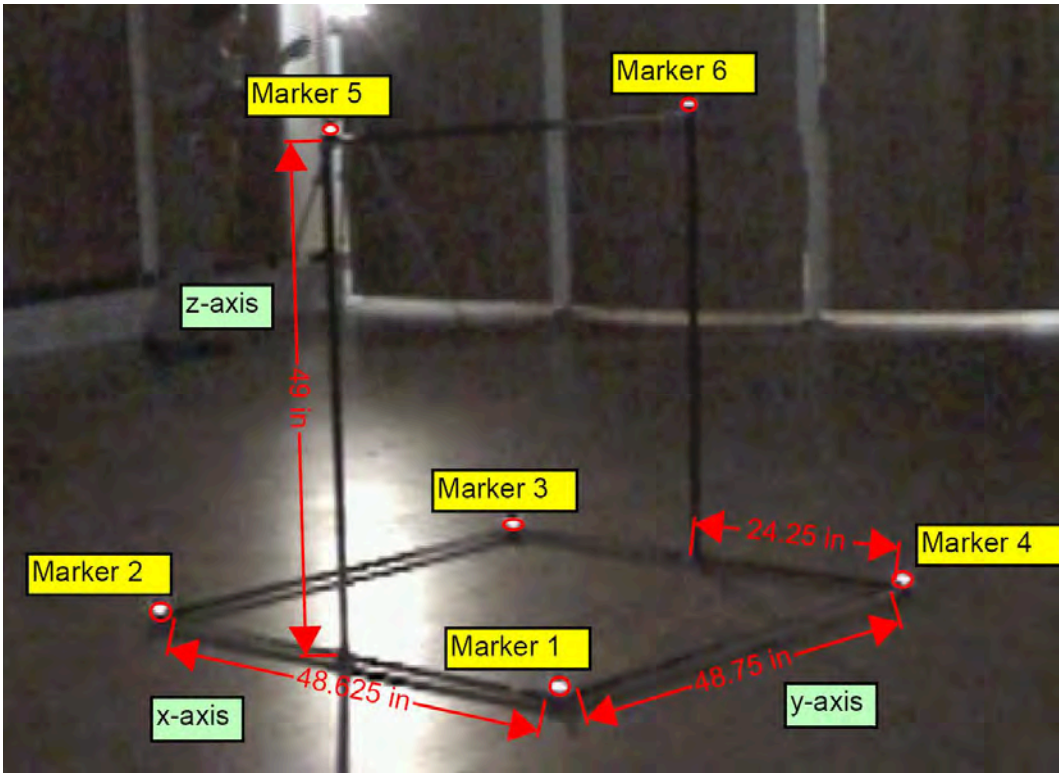

Figure 8.1: The structure that was used to calibrate the motion capture system.

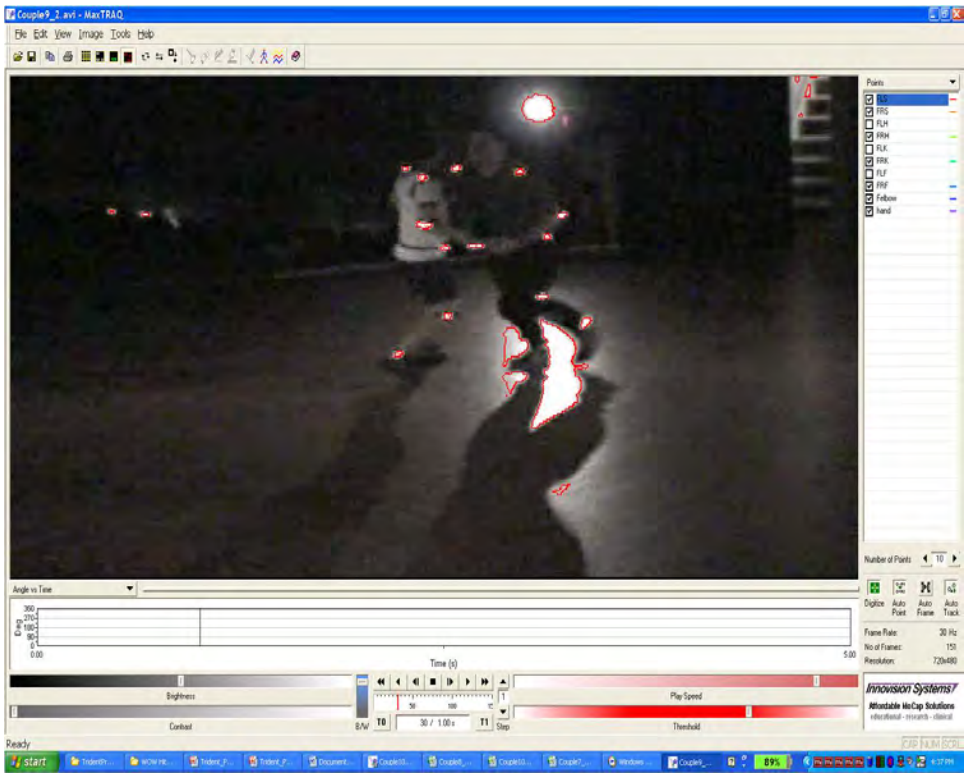

Figure 8.2: A screen capture of the view for tracking markers recorded in one camera. The markers in each of the four cameras must first be individidually tracked before they could be combined.

of the picture. Since system is not designed for use with spinning motions, we had to use a combination of auto-tracking and manual work to garner full tracking results. We chose the system because it was the best system in our price range, but in adapting it to our spin we are pushing the capabilities of the system. Figure 8.2 illustrates what the program looked like for tracking the markers in the video images from each of the four sessions. Additionally this picture illustrates the location of the markers on the body. Markers were placed at all of the joints of the body. Figure 8.3 shows how the program combines the four individual camera views to create the three dimensional data.

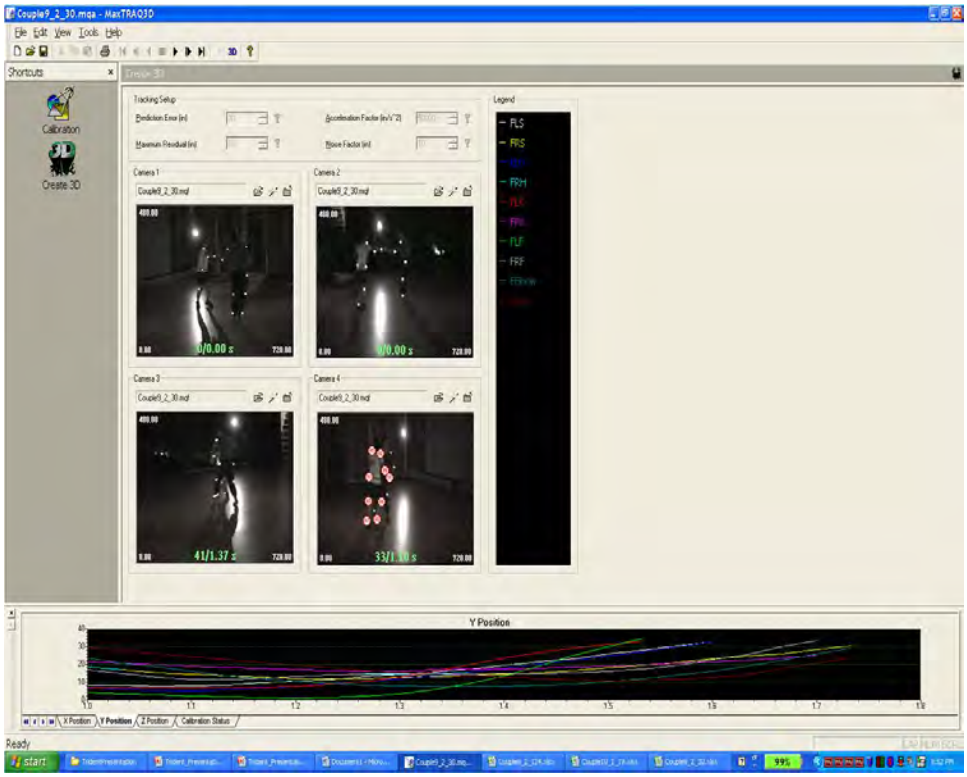

Figure 8.3: The view of the software for combining the four camera views to create a three dimensional image.

8.3 Procedures

8.3.1 Subject Selection

To conduct this research we used swing dancers with varying degrees of skill and experience. We drew from the population of midshipman and faculty dancers here at the Naval Academy and dancers in the general civilian population who live in the Baltimore/Washington/Annapolis area. The only considerations we made in selecting our research subjects is dance experience and availability to be recorded. Our expert dancers were all nationally regarded swing dance teachers and performers who have been dancing for five years or longer.

8.3.2 Data Recording

Dancers were given a consent form to sign and the purpose of the project and what they would be asked to do was also verbally explained to them. A copy of this consent form can be viewed in Appendix 2. They were then "suited up", which involved putting on all of the velcro straps that held the markers. Markers were place on each of the dancers ankles, knees, hips, shoulders, and their open elbows. An additional marker was placed on the follower's wrist and counted as the hand location for both dancers. Once the cameras were turned on and calibrated with the structure and a camera flash for timing, the dancers were asked to begin dancing and incorporate three to four rhythm circles or partnered spins into their dance. Participation took about 20 minutes per a couple.

8.3.3 Video Analysis

After the video was taken, I downloaded it to my computer. I converted it into audio video interleave (AVI) format, ensuring all the cameras were timed correctly, and breaking the large videos into smaller clips. The timing of the videos is particularly important because the four different cameras must be synchronized to capture a movement from all of the different angles. The clips needed to be small because the computer program that incorporates all of the data and synchronizes it cannot handle large amounts of data at one time. Once the data is in the system and the tracking is completed the MaxTraq program will output an excel spreadsheet with the X-Y-Z location in time of all of the points that were tracked. Tracking labels all the points in a given view so that MaxTraq can distinguish among the follower's elbow marker, the leader's shoulder marker, the follower's grind foot marker, et cetera. This data was then the output for models and the basis for building graphs to analyze the movement. To take the coordinate data and translate it into angles and representations of movements, we built vectors and used trigonometric calculations.

Chapter 9

Data Analysis and Results

9.1 Optimal and Achieved Acceleration

Our mathematical model predicts the achievable rotational acceleration for each pair of dancers in any fixed pose. Using numerical optimization we determined the best pose and corresponding highest rotational acceleration. The measurements of the pose the dancers actually used in their partnered spin are input into the same model to compute the achievable acceleration in that pose. We calculated a ratio of each couple's achievable acceleration in the observed pose to that of the optimal pose. A larger ratio means that the pair is achieving a higher fraction of their potential acceleration. Table 9.1 lists the achieved and optimal angular accelerations for each couple along with the fraction of optimal.

Couple H is not listed in the table because we were not able to garner reasonable data from the couple. Because of the pose in which they were standing and the limitations our model put on the rotation of the hip joint, Couple H's actual pose was entirely unreasonable by the definitions of our model. We did not observe this issue with any of the other couples recorded.

Since each dancer has different size parameters, the optimal poses and maximum achievable accelerations differ between the couples. We compared each couple's performance to their individual optimum. We hypothesized that the best couples would achieve a higher fraction of their optimum than less skilled dancers.

With our motion capture system, we could record an observed rotational acceleration. However, we still calculated an estimate of acceleration based on our simplified model, because we determined a fraction of optimal performance based on the optimal acceleration from the same model. Using the achievable acceleration in the actual

Achieved and Optimal Angular Acceleration				
Couple	Class	Achieved	Optimal	Fraction of Optimal
A	Expert	4.50093	45.9221	0.0980
B	Beginner	3.22323	44.6527	0.0722
C	Expert	6.44338	48.0171	0.1368
D	Beginner	3.49177	48.6595	0.0718
E	Expert	3.49527	49.8348	0.0701
F	Expert	4.972	47.3274	0.1056
G	Beginner	3.96729	49.8875	0.0795
I	Beginner	3.95054	45.0883	0.0876
J	Beginner	4.28396	42.431	0.1010

Table 9.1: Achievable and optimal acceleration for each couple and the fraction of optimal angular acceleration they achieved.

poses calculated from the same model provided a metric for comparing the couples' performances.

9.2 Statistical Analysis

To test our hypothesis, we used the Mann-Whitney statistical test to compare these numbers across couples. We first divided the couples into two categories, beginners and experts. The couples' fractions of optimal are then ranked from largest to smallest. With their ranks the fractions are then separated back into their categories and the ranks are summed together. This test is a one-tailed test, where we expect to find that if there is any difference between the categories, the experts will have a larger fraction of optimal. We set our significance level to $\alpha = .05$. Using a table from Rice's statistics book [11], we determined whether the two categories we ranked differed at a level of statistical significance. We did not find significant difference between the two categories.

Our small dataset may have contributed to our inability to find a significant difference between expert and beginner couples. We captured twenty different couples, but the couples pictured are the only ones we were able to process to output data from. A problem with calibrating our motion capture system caused a hang up in our data processing and as of now we have only processed the data from 10 couples. While we cannot reach any firm conclusions based on statistics, we can draw some interesting anecdotal observations based on the optimal poses that our model calculated.

All of our couple's optimal poses are very similar and seem intuitively logical. To spin fast the couples need to get close together and put their feet in close to the center of the circle. The push foot does need to have some distance to the axis of rotation so it can produce the torque required to initiate the spin. See Figures 9.1 - 9.9 for the actual and optimal poses for each couple.

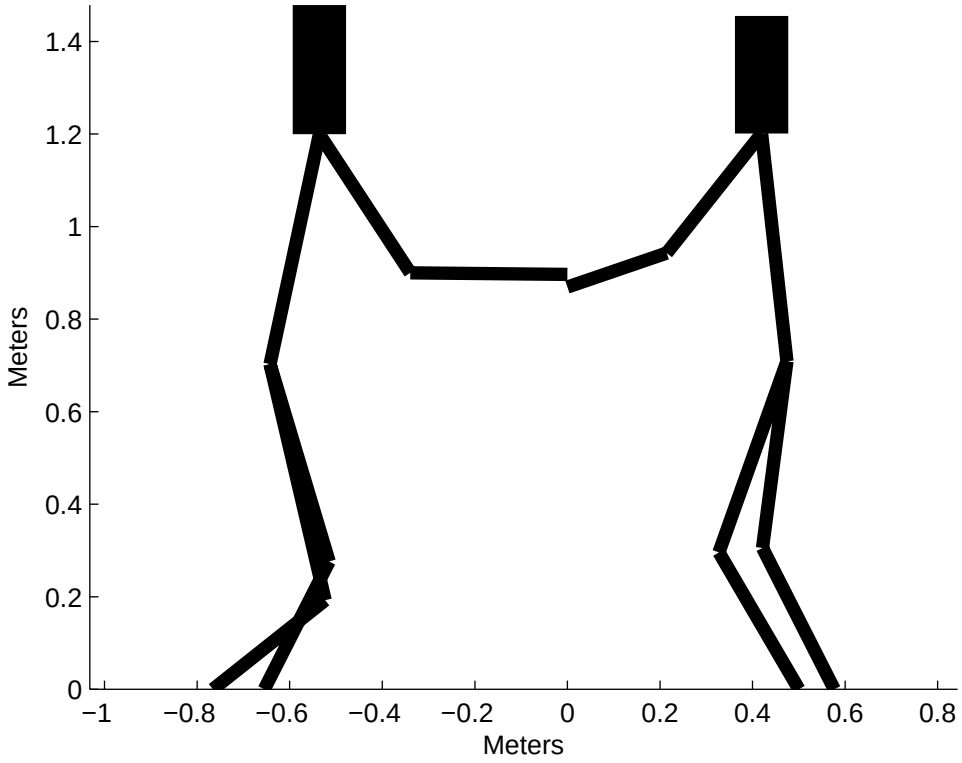

(a) The actual pose the dancers held

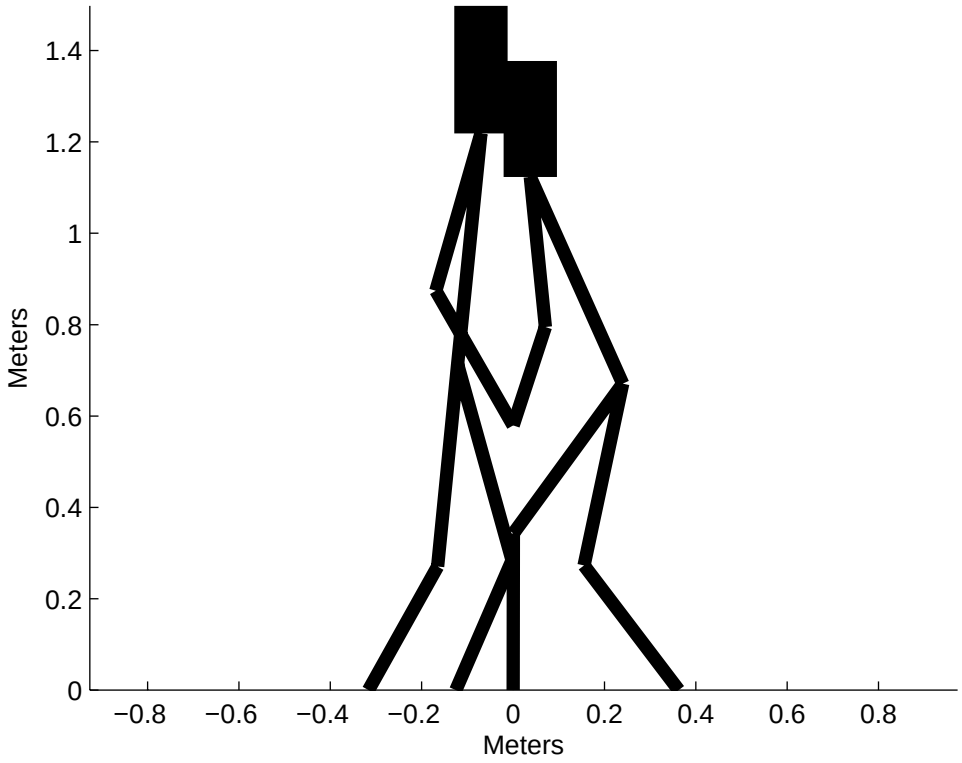

(b) The optimal pose as calculated by the model

Figure 9.1: The actual and optimal poses for couple A.

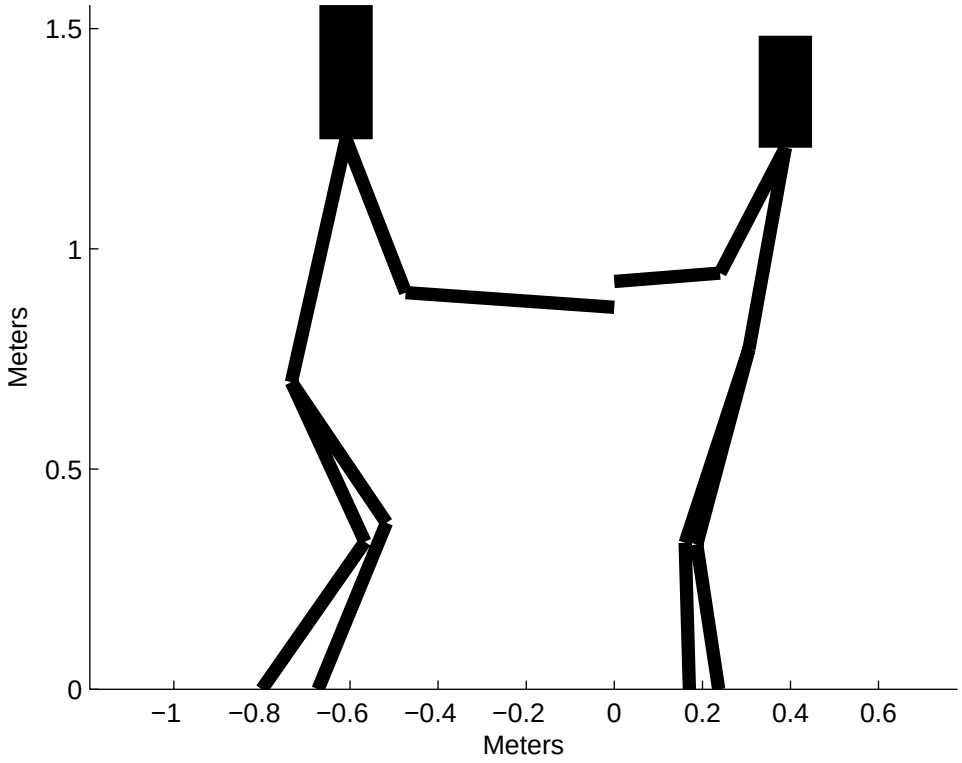

(a) The actual pose the dancers held

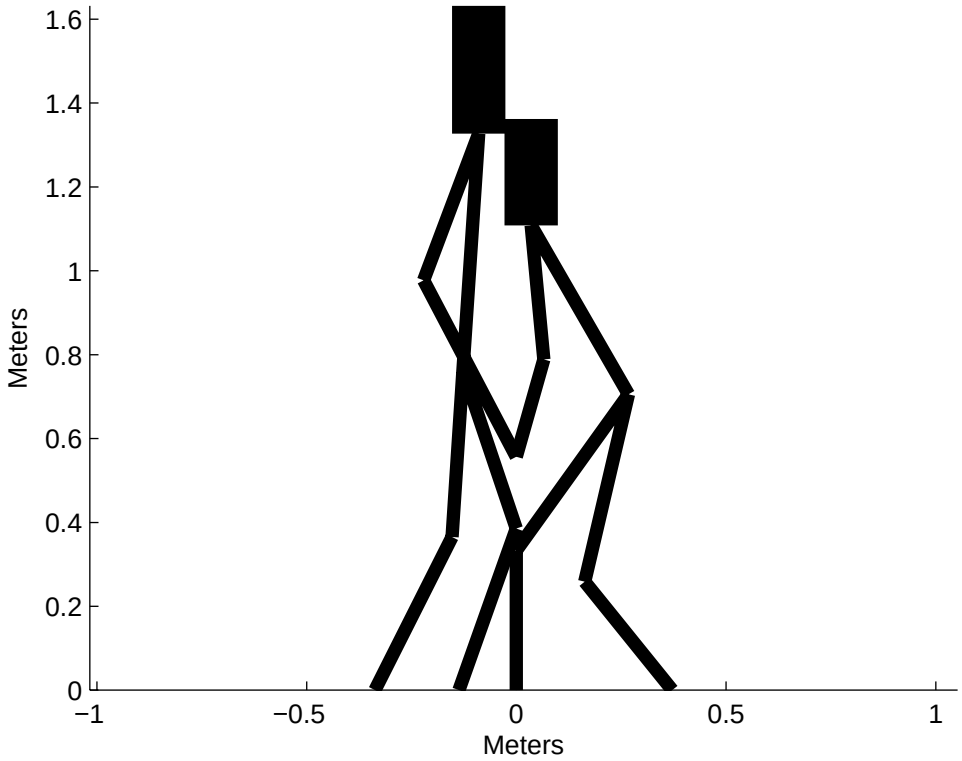

(b) The optimal pose as calculated by the model

Figure 9.2: The actual and optimal poses for couple B.

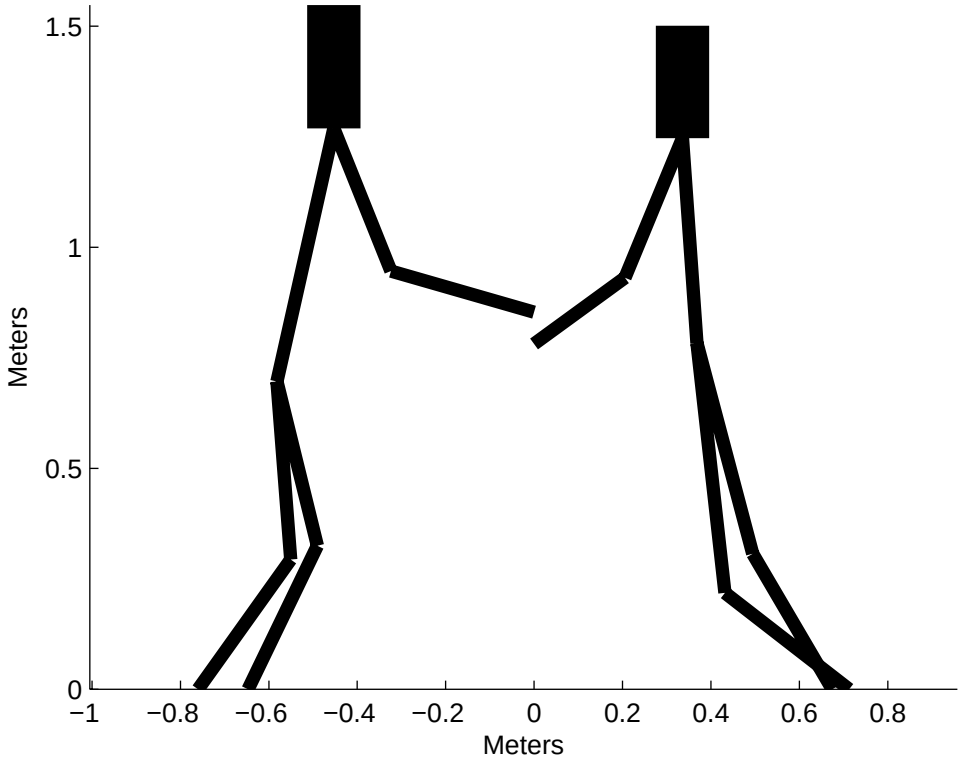

(a) The actual pose the dancers held

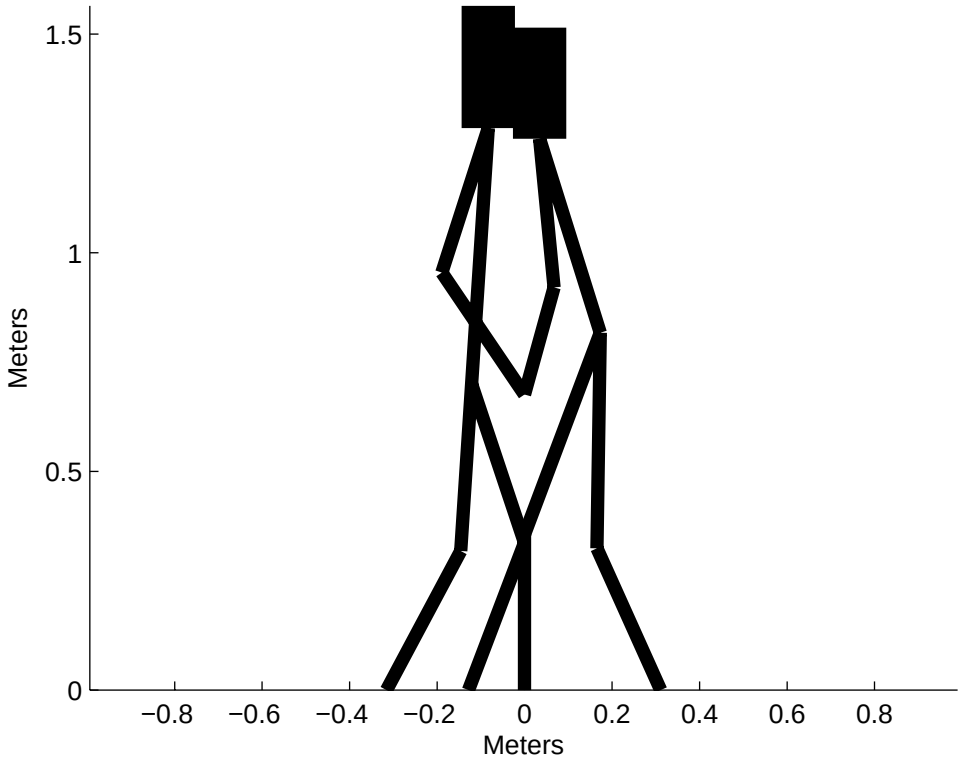

(b) The optimal pose as calculated by the model

Figure 9.3: The actual and optimal poses for couple C.

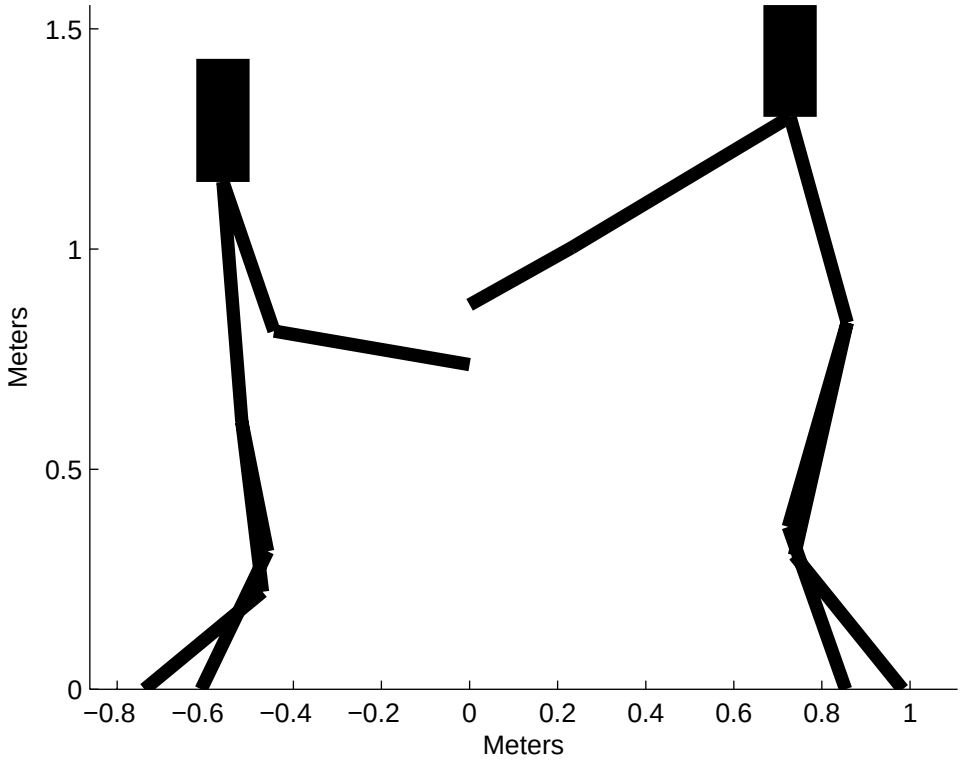

(a) The actual pose the dancers held

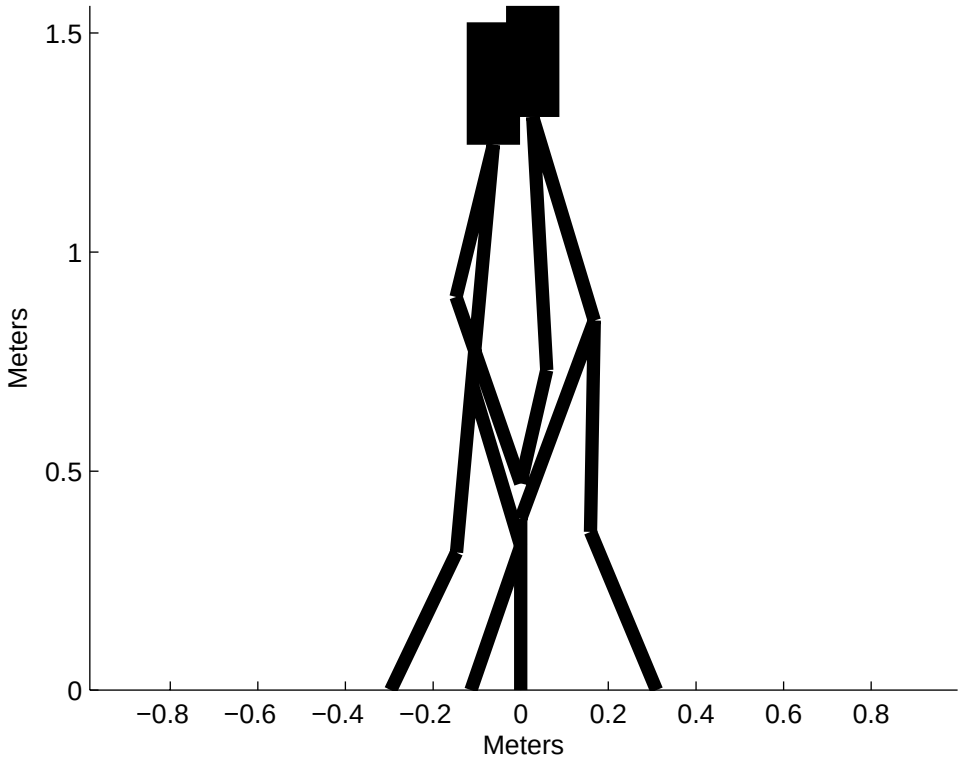

(b) The optimal pose as calculated by the model

Figure 9.4: The actual and optimal poses for couple D.

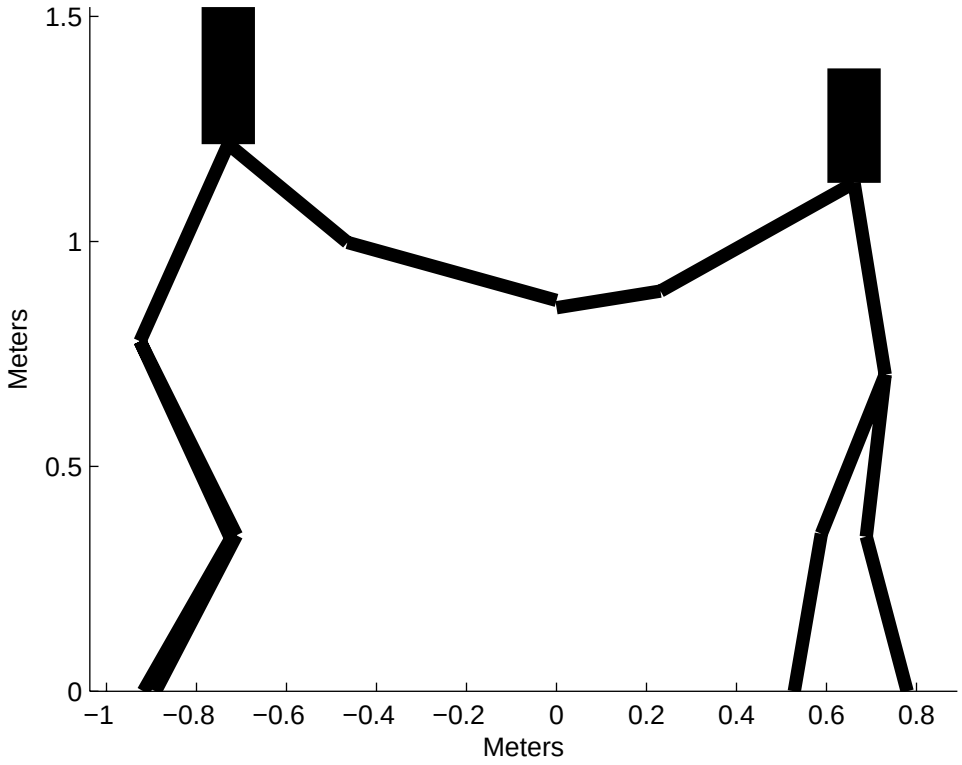

(a) The actual pose the dancers held

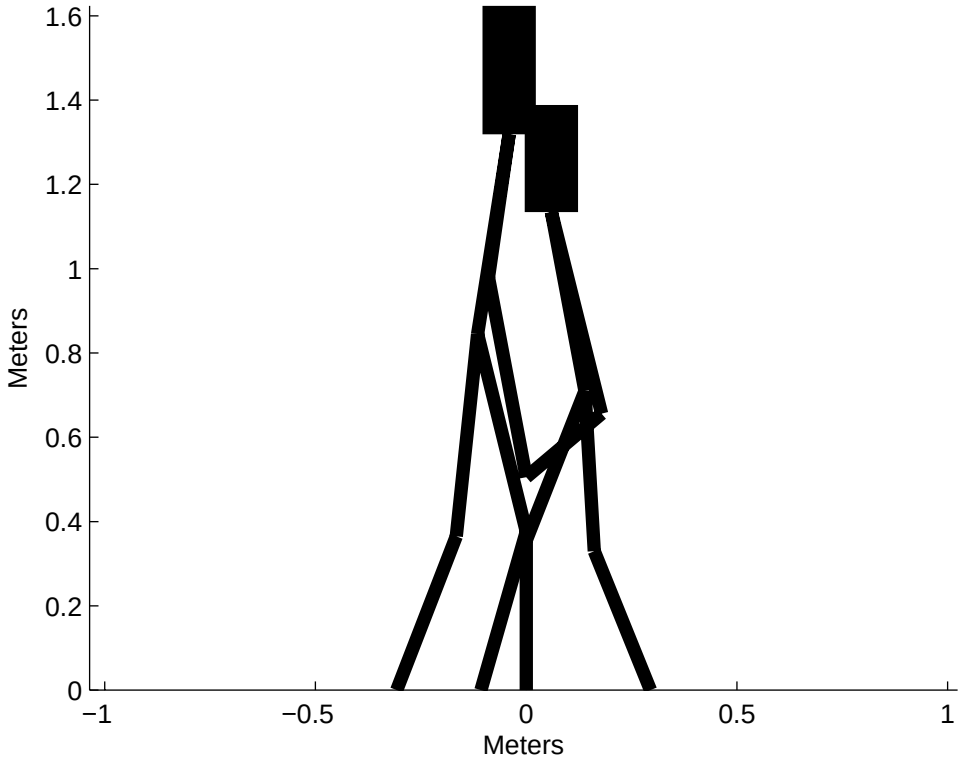

(b) The optimal pose as calculated by the model

Figure 9.5: The actual and optimal poses for couple E.

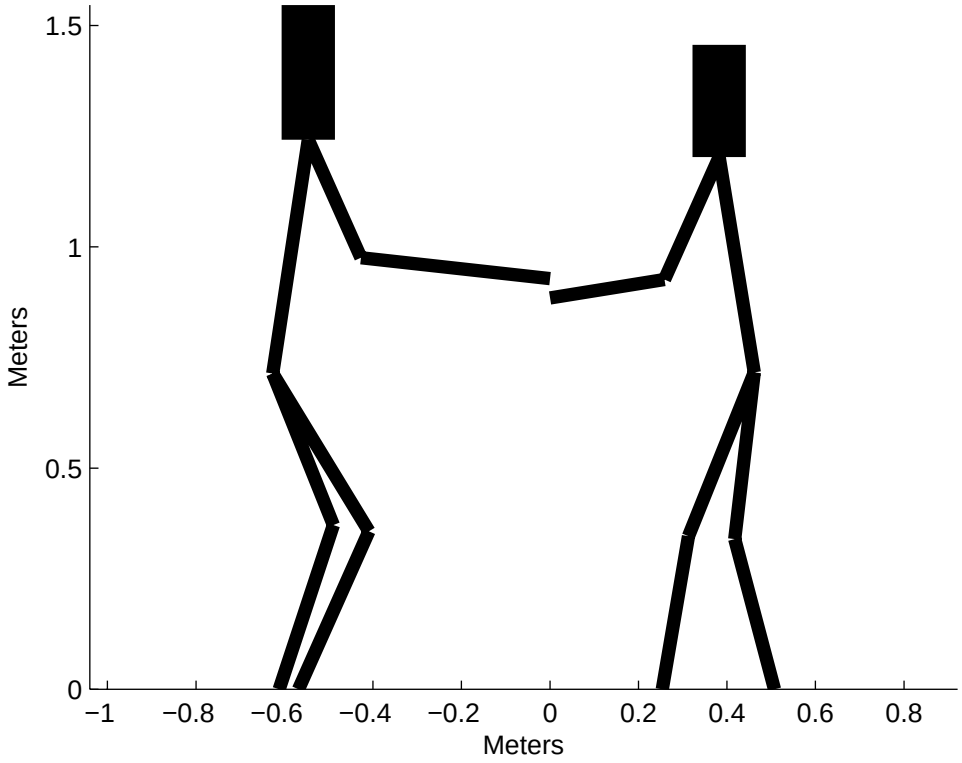

(a) The actual pose the dancers held

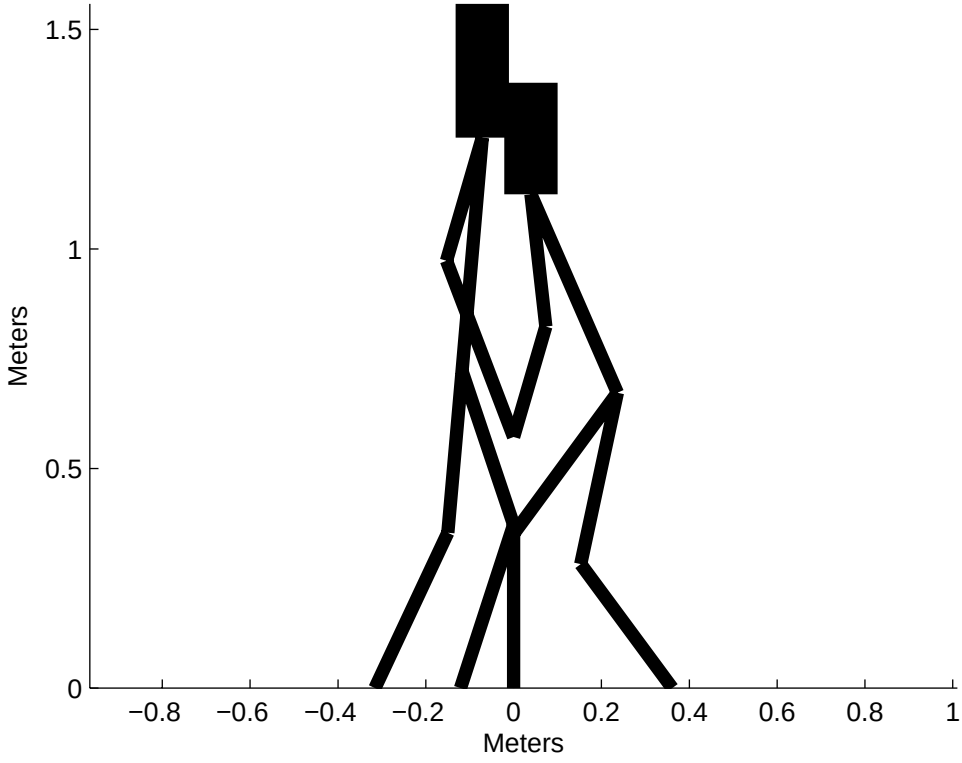

(b) The optimal pose as calculated by the model

Figure 9.6: The actual and optimal poses for couple F.

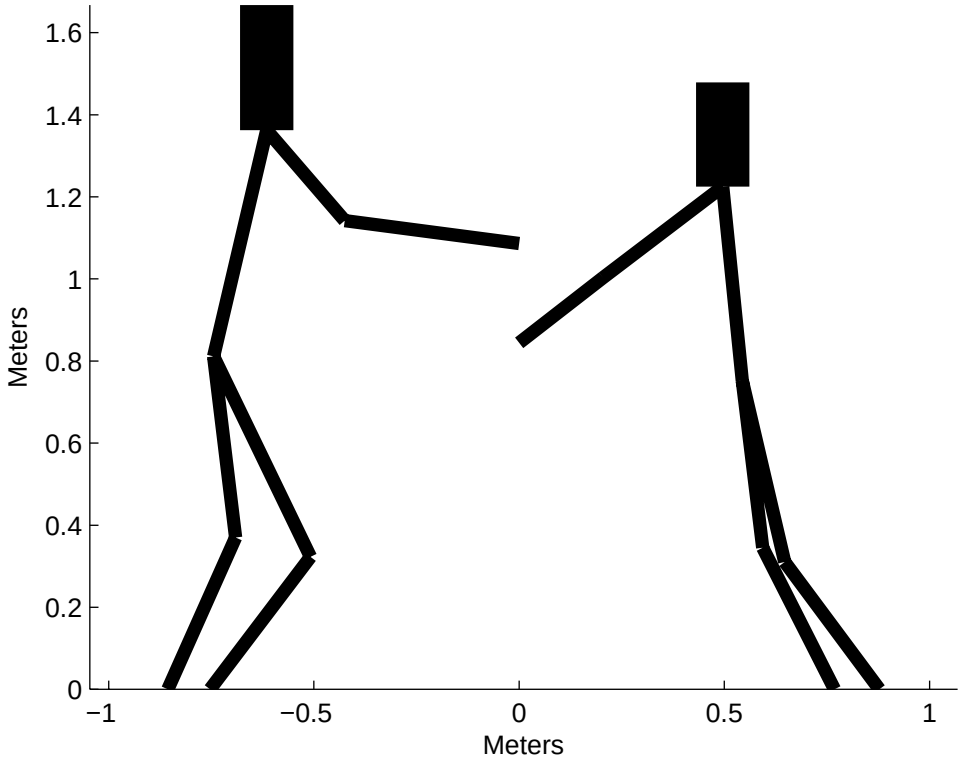

(a) The actual pose the dancers held

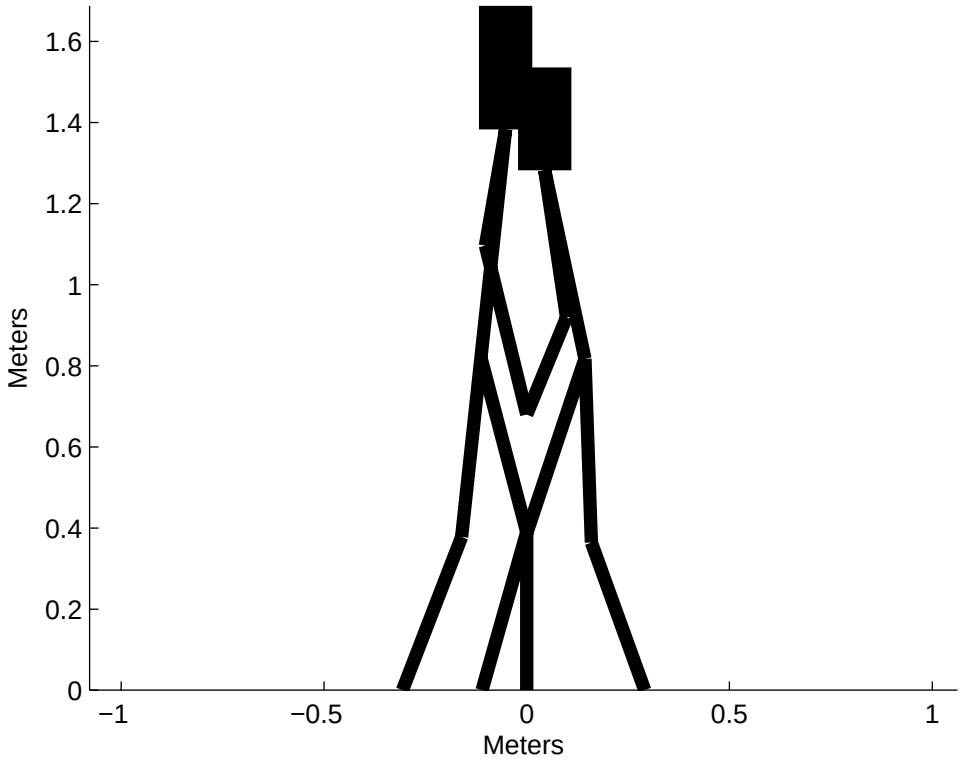

(b) The optimal pose as calculated by the model

Figure 9.7: The actual and optimal poses for couple G.

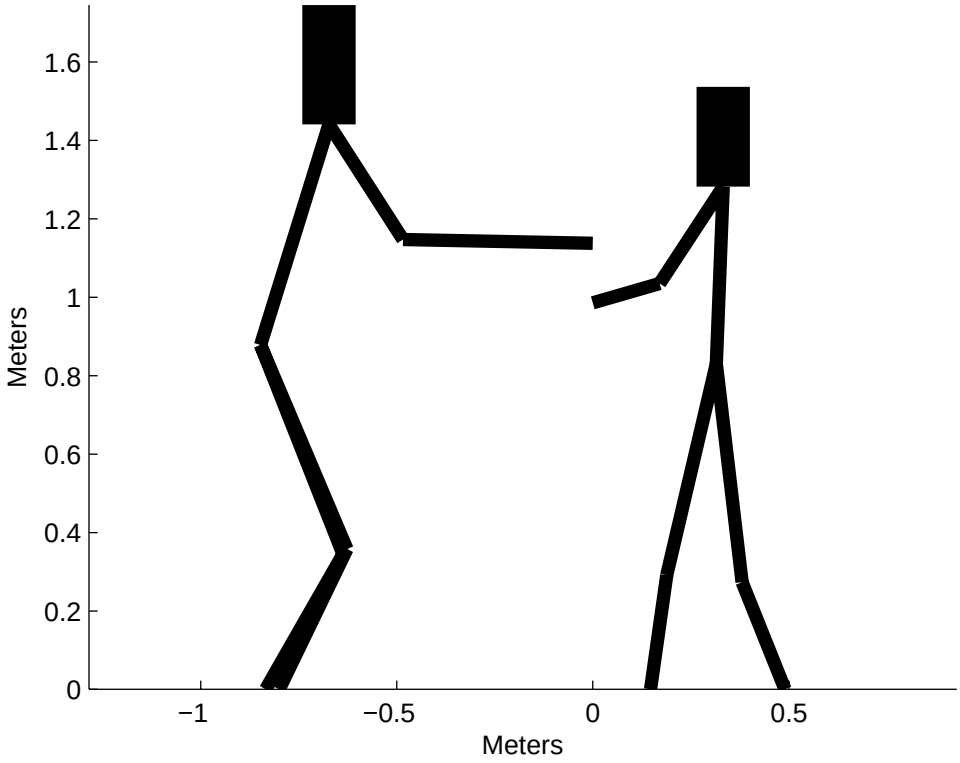

(a) The actual pose the dancers held

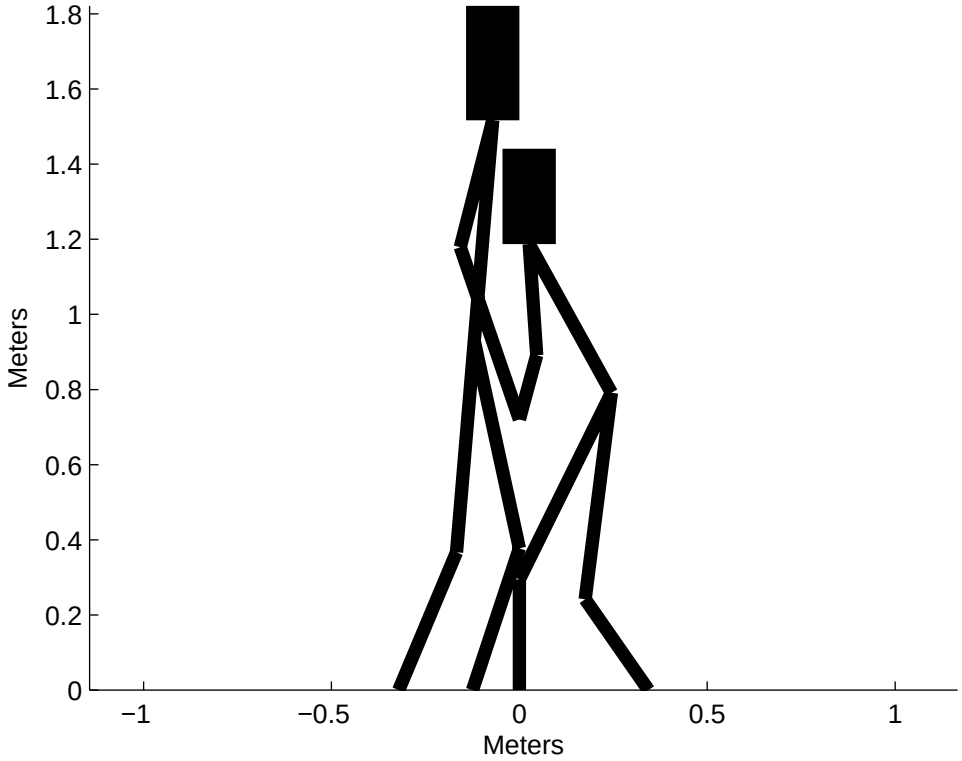

(b) The optimal pose as calculated by the model

Figure 9.8: The actual and optimal poses for couple I.

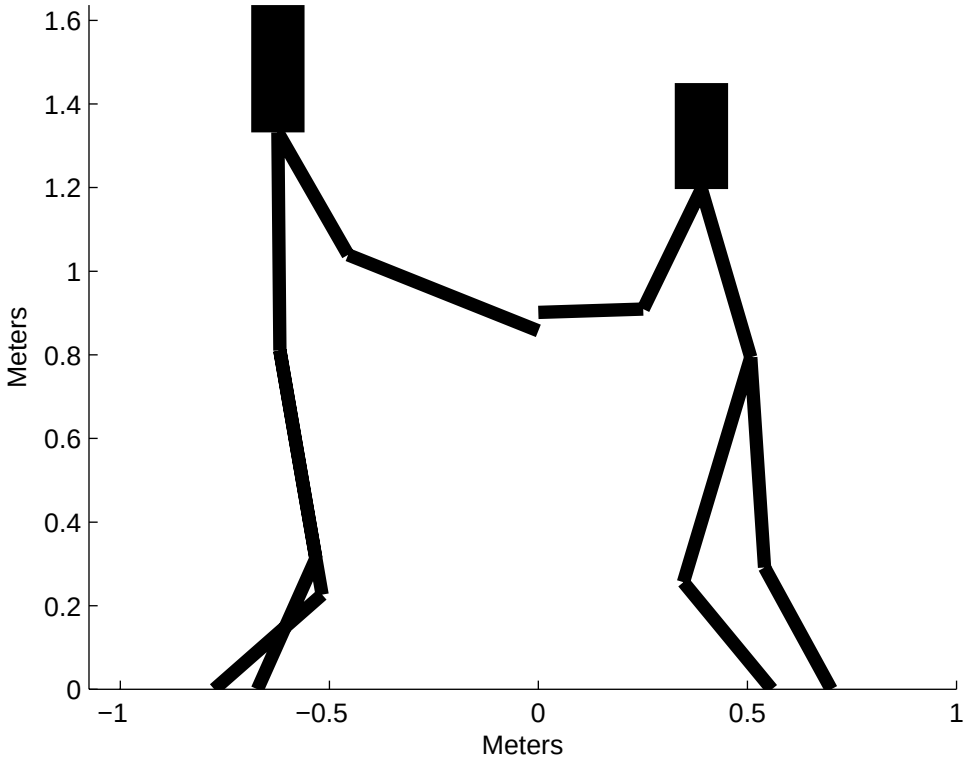

(a) The actual pose the dancers held

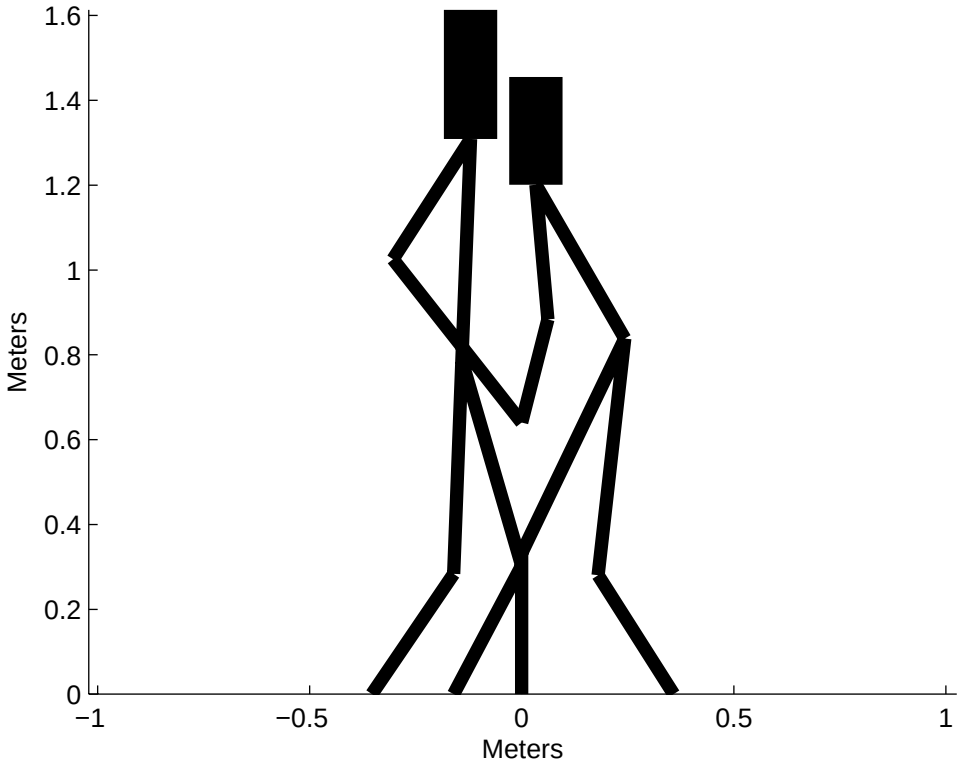

(b) The optimal pose as calculated by the model

Figure 9.9: The actual and optimal poses for couple J.

Chapter 10

Conclusion

10.1 Project Summary

In undertaking this work we hoped to understand the pose a swing dancer selects to complete a rhythm circle. We built a mathematical model to predict the optimal pose for a dance couple based on his and her specific size parameters. With this model we estimated the external forces on the system and the moment of inertia of the couple. With these values we calculated the angular acceleration of the couple and placed biologically reasonable constraints on the poses. Using an optimization algorithm we computed the "best" pose and compared it to the pose the couple actually held as shown from our motion capture system.

Analyzing our results, we find that the optimal pose predicted is logical. Qualitatively the optimum poses that we found are in very good agreement with what expert dancers would teach students about this partnered spin. Dance teachers usually advise that this spin works better the closer one can get to one's partner and that the right (grind) foot should be at or close to the axis of rotation while the left (push) foot should be farther away. Additionally, we were looking to determine if there was a difference between the fraction of optimal achieved by beginners and expert dancers. A statistically significant difference at the $\alpha = .05$ level was not found. The angular acceleration achieved by the couples was a factor of ten less than the predicted optimal acceleration. No couples in fact came close to their optimal acceleration. We examined a number of areas that might have been the cause of this large difference between achieved and optimal acceleration.

10.2 Model Shortcomings

In this project, we necessarily neglected a number of elements related to a partnered spin: the ease or difficulty with which people are able to hold various poses (internal forces), the need to see your partner, the more complicated arm connection points, the freedom of many joints like the shoulder and hip to move in more than a hinge fashion, the push versus grind phase of the spin, and the possibility that the dancers might be considering aesthetics instead of physics in their selection of a pose. Perhaps these simplifications explain why we saw none of the couples adopt a pose that is close to the optimal pose predicted by our model.

10.2.1 Hand Simplification

In retrospect, the decision to combine the various points of connection between the leader and follower into one link located at the leader's left and follower's right hand may have been pivotal. Recording the neglected closed arm connection, between the leader's right arm and the follower's back, would have made our "actual" poses seem much closer together than they appeared in our calculations. The closed arm around the back connection is generally considered a stronger and more useful connection in this type of spin and indeed in this dance than the connection at the open hands. By describing the dancers' actual performance in terms of the distance between their open hand-to-hand connection, we may have chosen a very noisy observation of the true distance between their torsos. Figure 10.1 illustrates the pose dancers spin in and shows how much closer the dancers are on their closed shoulder side. These dancers have a large distance between their open hands, which was the distance we considered for our model.

10.2.2 Dimensional Simplification

We began our project with a planar model and never completely moved past that model. In the future work should begin from a more complex three-dimensional model. While this might add more variables to an already complex problem, a more detailed model would allow for the full consideration of the closed position with a hand creating force at the shoulder and the other hand connecting to his partner. Additionally, a more biologically detailed three-dimensional model would allow "lean" in the pose, so a dancer might shift his or her weight in the y-direction to gain more torque.

When reviewing video and pictures of dancers we noticed that in some cases

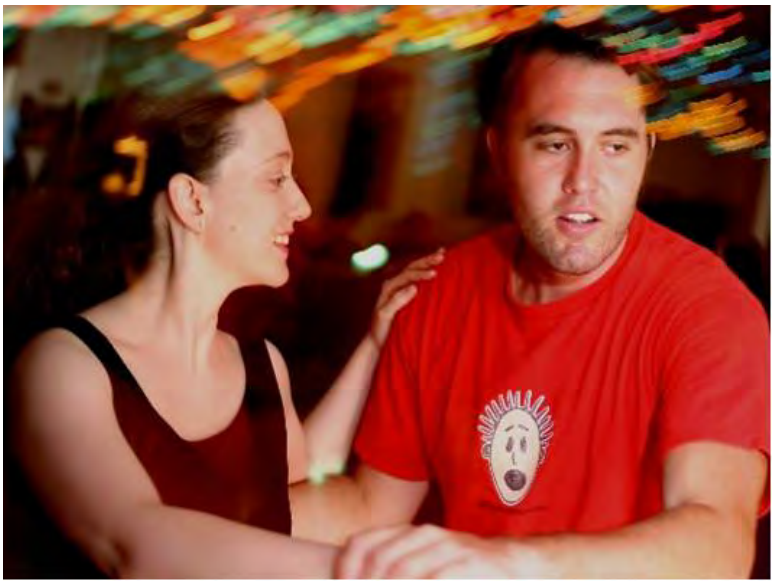

Figure 10.1: The pose dancers assume to spin. One arm is around their partners' shoulder (closed arm) and one grasping their partners' hand (open hand).

the dancers do not exactly face one another. The dancers' shoulders on the closed side, with the arm around the back connection, are much closer together than their shoulders on the open hand-to-hand connection side. Our model could not account for this twist. We could have partially addressed this limitation by examining the distance between the shoulders and making that the distance between the dancers. This technique would eliminate the consideration of the open hand.

10.2.3 Body Simplification

We treated the body as a collection of non-right cylinders. While we felt this simplification could provide us a reasonable answer, it also limited our ability to accurately model the data. A better model would have treated all of the body parts as stadiums and cones [8]. A stadium is a convex solid consisting of two halves of a truncated cone, separated by an appropriate-sized rectangular prism. This type of model would account for the shape of torso and positions of the legs because they would not be considered as strictly round cylinders. Additionally, the alternate model has been used by others so we would not have to construct it from first principles, as we did in this project.

10.3 Measuring Forces

Measuring forces might have simplified our problem. We attempted to estimate the forces the dancers applied, by relying completely on observations of a couple's pose. In the future, we might be able to use force sensors at the dancers' hands and on the floor to garner a much better picture of how hard the dancers were pushing and be able to incorporate that force into our model. By measuring the forces we eliminate the problem of calculating forces, and could instead further develop the body model to make it more physically realistic.

10.4 Optimization Shortcomings

We are unable to solve the system of equations for 27 variables to estimate the forces used to produce the spin. The sum of two of these unknown forces divided by total inertia defines a couple's angular acceleration, which we maximized. Because we could not solve the full problem, we created a surrogate method for estimating force based on the location of the dancer's center of mass over his or her push foot. In the future, further attempts might be made to estimate the forces based on the full problem instead of relying on a surrogate.

The optimization algorithm itself did not perform as well as we expected. The algorithm seems to be very sensitive to the initial search parameters and the optimal answer may change with even a slight change in initial search parameters. This sensitivity indicates that we got trapped in local optima instead of finding the global optimum. Because Mathematica owns the rights to the "NMaximize" algorithm we used, we are not able to analyze its methods to determine what might be going wrong. Future work in this area of the project could involve finding better programs for optimizing the pose or working on a different metric for determining best pose.

10.5 Lessons Learned

The data collection and analysis phase of this project took more time than expected. Our motion capture system had not been used previously at the Naval Academy. We had to be trained on the use of this system and work out some of the kinks ourselves. Due to the complexity of our motion and the drop-offs caused by the rotation, we had to use a combination of auto and manual tracking that is labor intensive. Once the model is tracked the output of the system is the three dimensional location of the

points. We took those locations and developed a method for calculating the angles and vectors of the pose. All of these processes took a considerable amount of time.

In repeating this project I would not rely so heavily on one software system. We used Mathematica for the vast majority of our calculations in this project. This program is useful because it allows us to maintain symbolic notation of our equations. While the program was useful in solving our simpler models, it was not able to provide us a reasonable solution to our fully developed model. We also relied heavily on the "NMaximize" function for our optimization. Toward the end of the project we looked into creating a Monte Carlo optimization scheme in Matlab, however, we did not have time to fully develop this method.

10.6 Accomplishments

One of the major accomplishments of this project is bringing a useful motion capture system to the Naval Academy. Prior to this project, no equipment or program for advanced motion capture study existed. The system setup we used for this project can track up to 24 points and handle very complex motions. Also, as a result of this project we have an archive of data of swing dancers, which later students could re-use.

We built a completely new model of a dance couple. Our model was not based on a previously developed model, but was literally built from the ground up. We defined the joint angles to draw an understanding of the pose the dancers were in and used the lengths of the actual couples' bodies to define the lengths of the model. To determine the optimal pose, we developed a method for estimating the forces at the feet and used an algorithm for maximizing the angular acceleration.

As a result of this model and the data collected we were able to perform a statistical significance test on ten couples to compare the fraction of optimal acceleration obtained by expert and beginning dancers. We also obtained images of the optimal poses that might be useful in helping dancers and dance teachers to better understand the optimal technique for spinning fast.

10.7 Future Work

While we have accomplished much this year, there is still more that could be done. One area for further research would be the development of a more advanced pose model. This work would be challenging because it would make a complicated problem

even more complex, but a more advanced model would allow for a much more accurate representation of the pose the couples assumed. Additionally, force sensors might be incorporated into future studies to gain a better picture of the actual forces involved in the spin. Our attempt to estimate the force strictly based on the pose was a major roadblock to the work we completed this year.

We did not consider the internal forces applied. The dancers are not reliant totally on external forces for producing spin, but generate force by contracting their muscles. Future work incorporating these forces might also yield more congruent results.

Finally, future studies could determine the best methods for solving this type of problem. Possibly a more high powered solver such as CPLEX needs to be used to garner good results. An entirely different technique for optimization, such as Monte Carlo might yield interesting results. Perhaps optimizing the angular acceleration is not the best metric for evaluating the dancers' poses. We assumed dancers were trying to spin fast, however, their objective might be to minimize muscular effort to spin or create a certain aesthetic quality. Our current objective also does not allow us to consider the full dynamic character of the motion or the steps the dancers took to create the spin. Further studies could consider the small changes in speed that occur within each rotation when the dancers take the steps required to produce rotation.

We could apply the same methods developed for the partnered spin to other motions. Particularly, an assisted jump could be an interesting application of further study of partnered movements. In addition to further swing dance applications, studying the interactions of wrestlers or people performing martial arts movements might be useful. Finally, using studies of optimal human motion towards the development of interactive robots would be an exciting area for future study.

Appendix 1: Code to Maximize α

See Chapters 3, 4, and 5 for descriptions of the notation for human body models used here. This appendix is the code for our mathematica program used to optimize angular acceleration.

Constants

```
inches2meters = 0.0254;
lbs2kgs = 0.4535923;
gravity = 9.8;
μs = 0.6;
fudge1 = 1.3;
frt = 30 inches2meters / (2 π);
frc = 15 inches2meters / (2 π);
frq = 20 inches2meters / (2 π);
frb = 10 inches2meters / (2 π);
frf = 7 inches2meters / (2 π);
frhead = 20 inches2meters / (2 π);
mrt = 36 inches2meters / (2 π)
mrc = 20 inches2meters / (2 π);
mrq = 24 inches2meters / (2 π);
mrb = 11 inches2meters / (2 π);
mrf = 8 inches2meters / (2 π);
mrhead = 24 inches2meters / (2 π);
```

Couple size parameters

```
fLb = 12.98 inches2meters;
fLf = 8.94 inches2meters;
fLt = 19.5 inches2meters;
fLq = 16 inches2meters;
fLc = 13.5 inches2meters;
fLhead = 10 inches2meters;
fMass = 127 lbs2kgs;
fmb = .0346 fMass;
fmf = .0163 fMass;
fmt = .615 fMass;
fmc = .059 fMass;
fmq = .183 fMass;
fmhead = .091 fMass;
mLb = 14.11 inches2meters;
mLf = 13.36 inches2meters;
mLt = 20 inches2meters;
mLq = 17.52 inches2meters;
mLc = 12.2 inches2meters;
mLhead = 11 inches2meters;
mMass = 230 lbs2kgs;
mmb = .0346 mMass;
mmf = .0163 mMass;
mmt = .615 mMass;
mmc = .059 mMass;
mmq = .183 mMass;
mmhead = .091 mMass;
```

Couple's actual recorded pose

```
θfb = .9;
θff = .33;
θffp = 2.04;
θffg = 2.1;
θfh = 1.46;
θfkp = 1.44;
θfkg = 1.2;

θmb = .99;
θmf = .01;
θmfg = 2.04;
θmfp = 2.47;
θmh = 1.36;
θmkg = 1.28;
θmkp = 1.3;
```

Range calculations

```
fRE = fLf Cos[θff];
fRs = fLb Cos[θfb] + fRE;
fRh = fRs + fLt Cos[θfh];
fRkg = fRh – fLq Cos[θfkg];
fRkp = fRh – fLq Cos[θfkp];
fRfg = fRkg – fLc Cos[θffg];
fRfp = fRkp – fLc Cos[θffp];
mRE = mLf Cos[θmf];
mRs = mLb Cos[θmb] + mRE;
mRh = mRs + mLt Cos[θmh];
mRkg = mRh – mLq Cos[θmkg];
mRkp = mRh – mLq Cos[θmkp];
mRfg = mRkg – mLc Cos[θmfg];
mRfp = mRkp – mLc Cos[θmfp];
```

Moment of inertia integrals

```
fInertiaHead = .5 fmhead frhead^2 + 0 + fRs^2 fmhead;
fInertiaBicep = .5 fmb frb^2 +
    1/12 (fmb fLb^2) Cos[θfb]^2 Sin[θfb] + (.5 fLb Cos[θfb] + fRE)^2 fmb;
fInertiaForearm = .5 fmf frf^2 + 1/12 (fmf fLf^2) Cos[θff]^2 Sin[θff] +
    (.5 fLf Cos[θff])^2 fmf;
fInertiaTorso = .5 fmt frt^2 + 1/12 (fmt fLt^2) Cos[θfh]^2 Sin[θfh] +
    (.5 fLt Cos[θfb] + fRs)^2 fmt;
fInertiaQuadGrind = .5 fmq frq^2 + 1/12 (fmq fLq^2) Cos[θfkg]^2 Sin[θfkg] +
    (fRh - .5 fLq Cos[θfkg])^2 fmq;
fInertiaCalfGrind = .5 fmc frc^2 + 1/12 (fmc fLc^2) Cos[θffg]^2 Sin[θffg] +
    (fRkg - .5 fLc Cos[θffg])^2 fmc;
fInertiaQuadPush = .5 fmq frq^2 + 1/12 (fmq fLq^2) Cos[θfkp]^2 Sin[θfkp] +
    (fRh - .5 fLq Cos[θfkp])^2 fmq;
fInertiaCalfPush = .5 fmc frc^2 + 1/12 (fmc fLc^2) Cos[θffp]^2 Sin[θffp] +
    (fRkg - .5 fLc Cos[θffp])^2 fmc;

fInertiaTotal = fInertiaHead + fInertiaTorso +
   fInertiaQuadGrind + fInertiaCalfGrind + fInertiaQuadPush +
   fInertiaCalfPush + 2 fInertiaBicep + 2 fInertiaForearm;

mInertiaHead = .5 mmhead mrhead^2 + 0 + mRs^2 mmhead;
mInertiaBicep = .5 mmb mrb^2 +
```

$$\frac{1}{12}\left(\text{mmb mLb}^2\right)\text{Cos}[\theta\text{mb}]^2\,\text{Sin}[\theta\text{mb}] + (.5\,\text{mLb Cos}[\theta\text{mb}] + \text{mRE})^2\,\text{mmb};$$

$$\text{mInertiaForearm} = .5\,\text{mmf mrf}^2 + \frac{1}{12}\left(\text{mmf mLf}^2\right)\text{Cos}[\theta\text{mf}]^2\,\text{Sin}[\theta\text{mf}] + (.5\,\text{mLf Cos}[\theta\text{mf}])^2\,\text{mmf};$$

$$\text{mInertiaTorso} = .5\,\text{mmt mrt}^2 + \frac{1}{12}\left(\text{mmt mLt}^2\right)\text{Cos}[\theta\text{mh}]^2\,\text{Sin}[\theta\text{mh}] + (.5\,\text{mLt Cos}[\theta\text{mb}] + \text{mRs})^2\,\text{mmt};$$

$$\text{mInertiaQuadGrind} = .5\,\text{mmq mrq}^2 + \frac{1}{12}\left(\text{mmq mLq}^2\right)\text{Cos}[\theta\text{mkg}]^2\,\text{Sin}[\theta\text{mkg}] + (\text{mRh} - .5\,\text{mLq Cos}[\theta\text{mkg}])^2\,\text{mmq};$$

$$\text{mInertiaCalfGrind} = .5\,\text{mmc mrc}^2 + \frac{1}{12}\left(\text{mmc mLc}^2\right)\text{Cos}[\theta\text{mfg}]^2\,\text{Sin}[\theta\text{mfg}] + (\text{mRkg} - .5\,\text{mLc Cos}[\theta\text{mfg}])^2\,\text{mmc};$$

$$\text{mInertiaQuadPush} = .5\,\text{mmq mrq}^2 + \frac{1}{12}\left(\text{mmq mLq}^2\right)\text{Cos}[\theta\text{mkp}]^2\,\text{Sin}[\theta\text{mkp}] + (\text{mRh} - .5\,\text{mLq Cos}[\theta\text{mkp}])^2\,\text{mmq};$$

$$\text{mInertiaCalfPush} = .5\,\text{mmc mrc}^2 + \frac{1}{12}\left(\text{mmc mLc}^2\right)\text{Cos}[\theta\text{mfp}]^2\,\text{Sin}[\theta\text{mfp}] + (\text{mRkg} - .5\,\text{mLc Cos}[\theta\text{mfp}])^2\,\text{mmc};$$

$$\text{mInertiaTotal} = \text{mInertiaHead} + \text{mInertiaTorso} + \text{mInertiaQuadGrind} + \text{mInertiaCalfGrind} + \text{mInertiaQuadPush} + \text{mInertiaCalfPush} + 2\,\text{mInertiaBicep} + 2\,\text{mInertiaForearm};$$

$$\text{InertiaTotal} = \text{fInertiaTotal} + \text{mInertiaTotal};$$

Location of joints calculation

```
fHkg = fLc Sin[θffg];
fHkp = fLc Sin[θffp];
fHh = fHkg + fLq Sin[θfkg];
fHhip = fHkp + fLq Sin[θfkp];
fHs = fHh + fLt Sin[θfh];
fHE = fHs – fLb Sin[θfb];
fHhand = fHE – fLf Sin[θff];
mHkg = mLc Sin[θmfg];
mHkp = mLc Sin[θmfp];
mHh = mHkg + mLq Sin[θmkg];
mHhip = mHkp + mLq Sin[θmkp];
mHs = mHh + mLt Sin[θmh];
mHE = mHs – mLb Sin[θmb];
mHhand = mHE – mLf Sin[θmf];
```

Center of mass calculation

$$fxCoMf = \frac{fRE}{2};$$

$$fxCoMb = \frac{fRE + fRs}{2};$$

$$fxCoMt = \frac{fRh + fRs}{2};$$

$$fxCoMqg = \frac{fRh + fRkg}{2};$$

$$fxCoMqp = \frac{fRh + fRkp}{2};$$

$$fxCoMcg = \frac{fRfg + fRkg}{2};$$

$$fxCoMcp = \frac{fRfp + fRkp}{2};$$

$$fxCoM = \frac{1}{fMass}\,(2\,fmb\,fxCoMb + fmc\,fxCoMcg + fmc\,fxCoMcp + 2\,fmf\,fxCoMf + fmq\,fxCoMqg + fmq\,fxCoMqp + fmt\,fxCoMt)$$

$$mxCoMf = -\frac{mRE}{2};$$

$$mxCoMb = -\frac{1}{2}\,(mRE + mRs);$$

$$mxCoMt = -\frac{1}{2}\,(mRh + mRs);$$

$$mxCoMqg = -\frac{1}{2}\,(mRh + mRkg);$$

$$mxCoMqp = -\frac{1}{2}\,(mRh + mRkp);$$

$$mxCoMcg = -\frac{1}{2}\,(mRfg + mRkg);$$

$$mxCoMcp = -\frac{1}{2}\,(mRfp + mRkp);$$

$$mxCoM = \frac{1}{mMass}\,(2\,mmb\,mxCoMb + mmc\,mxCoMcg + mmc\,mxCoMcp + 2\,mmf\,mxCoMf + mmq\,mxCoMqg + mmq\,mxCoMqp + mmt\,mxCoMt);$$

$$fzCoMcg = \frac{fHkg}{2};$$

$$fzCoMcp = \frac{fHkp}{2};$$

$$fzCoMqg = \frac{fHh + fHkg}{2};$$

$$fzCoMqp = \frac{fHh + fHkp}{2};$$

$$fzCoMt = \frac{fHs + fHh}{2};$$

$$fzCoMb = \frac{fHs + fHE}{2};$$

$$fzCoMf = \frac{fHE + fHh}{2};$$

$$fzCoM = \frac{1}{fMass}\,(2\,fmf\,fzCoMf + 2\,fmb\,fzCoMb + fmt\,fzCoMt + fmq\,fzCoMqg + fmq\,fzCoMqp + fmc\,fzCoMcg + fmc\,fzCoMcp);$$

$$mzCoMcg = \frac{mHkg}{2};$$

$$mzCoMcp = \frac{mHkp}{2};$$

$$mzCoMqg = \frac{mHh + mHkg}{2};$$

$$mzCoMqp = \frac{mHh + mHkp}{2};$$

$$mzCoMt = \frac{mHs + mHh}{2};$$

$$mzCoMb = \frac{mHs + mHE}{2};$$

$$mzCoMf = \frac{mHE + mHh}{2};$$

$$mzCoM = \frac{1}{mMass}\,(2\,mmf\,mzCoMf + 2\,mmb\,mzCoMb + mmt\,mzCoMt + mmq\,mzCoMqg + mmq\,mzCoMqp + mmc\,mzCoMcg + mmc\,mzCoMcp);$$

Alpha, from surrogate for generated force from push foot

$$\text{fDistPush} = \sqrt{(\text{fxCoM} - \text{fRfp})^2 + \text{frt}^2};$$

$$\text{fDistGrind} = \sqrt{(\text{fxCoM} - \text{fRfg})^2 + \text{frt}^2};$$

$$\text{fWeightPush} = \frac{\text{fDistGrind}}{\text{fDistGrind} + \text{fDistPush}};$$

$$\text{fNormalPush} = \text{fWeightPush}\ \text{fMass}\ \text{gravity};$$

$$\text{fForce} = \text{fRfp}\ \text{fNormalPush}\ \mu\text{s};$$

$$\text{mDistPush} = \sqrt{(\text{mxCoM} - \text{mRfp})^2 + \text{mrt}^2}$$

$$\text{mDistGrind} = \sqrt{(\text{mxCoM} - \text{mRfg})^2 + \text{mrt}^2}$$

$$\text{mWeightPush} = \frac{\text{mDistGrind}}{\text{mDistGrind} + \text{mDistPush}}$$

$$\text{mNormalPush} = \text{mWeightPush}\ \text{mMass}\ \text{gravity};$$

$$\text{mForce} = \text{mRfp}\ \text{mNormalPush}\ \mu\text{s};$$

$$\text{Alpha} = \frac{\text{mForce} + \text{fForce}}{\text{InertiaTotal}};$$

Optimize estimated rotational acceleration subject to biologically reasonable pose constraints

```
NMaximize[{Alpha, θmh + θmkg ≤ π, θmh + θmkp ≤ π, θmkp - θmfp ≤ 0,
  θmkg - θmfg ≤ 0, θmh > π/3, mRfg ≥ 0, mRfp ≥ 0, mRkg ≥ 0, mRkp ≥ 0,
  mRh ≥ 0, mRs ≥ 0, mRE ≥ 0, θfh + θfkg ≤ π, θfh + θfkp ≤ π,
  θfkp - θffp ≤ 0, θfkg - θffg ≤ 0, θfh > π/3, fRfg ≥ 0, fRfp ≥ 0,
  fRkg ≥ 0, fRkp ≥ 0, fRh ≥ 0, fRs ≥ 0, fRE ≥ 0, fHhand - mHhand == 0,
  fHh - fHhip == 0, mHh - mHhip == 0, fxCoM - fRfg ≥ 0,
  -mxCoM - mRfg ≥ 0, θff - θfb ≤ 0, θmf - θmb ≤ 0, θfb ≥ 0, θmb ≥ 0},
 {{θfb, .8, 1}, {θff, .2, .4}, {θffg, 2, 2.2}, {θffp, 2.0, 2.1},
  {θfh, 1.4, 1.50}, {θfkg, 1.1, 1.3}, {θfkp, 1.4, 1.6},
  {θmb, .8, 1}, {θmf, .2, .4}, {θmfg, 2.0, 2.1}, {θmfp, 2, 2.2},
  {θmh, 1.4, 1.50}, {θmkg, 1.4, 1.6}, {θmkp, 1.1, 1.3}}]
```

```
{45.9221, {θfb → 1.67042, θff → 1.25533, θffg → 1.5708,
  θffp → 2.22054, θfh → 1.14993, θfkg → 0.939004,
  θfkp → 1.36497, θmb → 1.85173, θmf → 1.05439, θmfg → 1.97976,
  θmfp → 2.08189, θmh → 1.46988, θmkg → 1.29923, θmkp → 1.67172}}
```

Appendix 2: Human Subjects Research Approval and Consent Form

25 September 2008

MEMORANDUM

From: Ms. Erin Johnson, Academy's HRPP Office

To: MIDN Megan Selbach-Allen, Trident Scholar

Subject: APPROVAL OF HUMAN SUBJECT RESEARCH

Ref: (a) SECNAVINST 3900.39D
(b) 32 CFR 219
(c) USNA HRPP Policy Manual

USNA Assurance # DoD N-40052

1. The Superintendent, as the Institutional Signatory Official (ISO), approved your research protocol "Mathematical Applications of Physics Principles to Swing Dance" involving human subjects.
   a. The approval date is 22 September 2008. The approval is in effect for one year.
   b. The approval will expire on 21 September 2009.
   c. If the research is to be continued beyond 21 September 2009, please submit your renewal application to this office by 21 August 2009 to allow time for adequate processing.

2. The HRPP Approval on this protocol # is **USNA.2008.0064-IR-EP7-A**. Please be sure to reference this number on any official correspondence regarding this proposal. The research is considered expedited according to reference (b) as research on individual or group characteristics. (Category 7)

3. Per the USNA HRPP Policy and Procedures manual (Section X), if there should be any changes to the design or methodology of your proposal, you must submit an amendment to your application in sufficient time to process the revisions and secure approval of the ISO.

4. You are required to report when the research has concluded according to Section XIII of the USNA HRPP Policy and Procedures manual and to provide this office with copies of any articles or presentations resulting from this research. Additionally, any presentations or publications must include acknowledgement of IRB approval using the HRPP approval number.

5. If you have any questions, please contact this office at 410-293-2533 or HRPPoffice@usna.edu.

ERIN JOHNSON
Academy's HRPP Office

Swing Dance Experiment Agreement
United States Naval Academy Department of Mathematics

The purpose of this research is to gain insight into how human beings apply physics principles in their dancing. In particular, we are developing a mathematical model that might predict good poses for rhythm circles, and we would like to see whether our predictions match the way people dance. Rhythm circles are our testbed for ideas about pose during the 3 and 4 (the closed position counts) of a swingout.

As a participant in this study I volunteer one hour of my time. During this time I understand that I will be weighed and measured to determine my height and the dimensions of my legs, arms and torso. I also consent to being interviewed about my dance background and views on how my dancing is affected by physical considerations. Finally, I will be marked with bright colored sensors and videotaped as I dance with my partner.

I understand that my name and contact information will never be disclosed. My name and contact information will be kept in a key locked file cabinet located in a code locked room. The only people who will have access to this information will be the primary investigator, MIDN Megan Selbach-Allen (m095835@usna.edu), and the two co-investigators Asst. Professor Sommer Gentry (gentry@usna.edu) and Assoc. Professor Kevin McIlhany (mcillhany@usna.edu). All the data collected in this experiment will be kept in the same secure location until it is incorporated into reported results.

I understand that in undertaking this study I am incurring some risks. These risks include the potential for embarrassment or discomfort from being recorded during my dancing. Also, I understand that when performing any physical activity there is some risk of injury. I will not hold the US Navy or the researchers responsible if an injury occurs, unless the injury is a result of the researchers' negligence.

I also understand that there are benefits to my participation such as a feeling of satisfaction for contributing to the scientific understanding of dance. Also, I will be video taped dancing and will have the opportunity to view my tape, which might provide insights that would allow me to improve my dancing. I can also view the results of the research available in the summer of 2009.

I am participating in this experiment voluntarily. I give my consent for the following to be used for the purpose of the study and any reports of results of this study: the measured motion and position data acquired today, my measured physical dimensions, my interview responses, and the video record of today's study. I may withdraw from the study at any time without negative

consequence. If I decide to withdraw from the study after data has been collected, my data will be destroyed and further publication of that data prevented.

I understand that I may also contact the Chair of the Math Department at the U.S. Naval Academy, Professor Tom Sanders, at 410-293-6702 if I have questions about the research practices of the investigator. I may contact the Human Research Protections Program office at the U.S. Naval Academy at HRPPoffice@usna.edu, if I have questions about my rights or any research-related injuries. The reference tracking number attached to this research project is USNA.2008.0064-IR-EP7-A.

Describe your swing dancing experience (number of years, number of times per week):

_____

_____

Describe your swing dancing skill level (beginner, intermediate, expert, world champion):

_____

_____

Print Name: _____

Signature: _____

Date: _____

If you would like a copy of the final report, please provide an email address below.

_____

Bibliography

[1] Office of Naval Research Broad Agency Announcement: Multi-disciplinary basic research in the science of autonomy with naval relevance, 2008.

[2] Baoming Ma Christine C. Raasch, Felix E. Zajac and William S. Levine. Muscle coordination of maximum-speed pedaling. *Journal of Biomechanics*, 30:595–602, 1997.

[3] Sommer E. Gentry. *Dancing cheek to cheek: Haptic communication between partner dancers and swing as a finite state machine*. PhD thesis, Massachusetts Institute of Technology, Cambridge, MA, 2005.

[4] H. Hatze. The complete optimization of a human motion. *Mathematical Biosciences*, 28:99–135, 1976.

[5] Kenneth Laws. Momentum transfer in dance. *Medical Problems of Performing Artists*, 13(136–145), 1998.

[6] Kenneth Laws. *Physics and the art of dance Understanding movement*. Oxford University Press, Mar 2005.

[7] Gergana Stefanova Nikolova and Yuli Emilov Toshev. Estimation of male and female body segment parameters of the bulgarian population using a 16-segmental mathematical model. *Journal of Biomechanics*, 40:3700–3707, 2007.

[8] Michael J. Pavol, Tammy M. Owings, and Mark D. Grabiner. Body segment inertial parameter estimation for the general population of older adults. *Journal of Biomechanics*, 35:707–712, 2002.

[9] Timothy J. Pennings. Do dogs know calculus? *The College Mathematics Journal*, 34(3):178–182, 2003.

[10] Janos D. Pinter. *Applied Nonlinear Optimization in Modeling Environments*, chapter Software Implementations for Compilers, Spreadsheets, Modeling Languages, and Integrated Computing Systems, pages 149–173. CRC Press Inc., 2007.

[11] John Rice. *Mathematical Statistics and Data Analysis*. Duxbury Press, 1995.

[12] Alla Safanova, Jessica K. Hodgkins, and Nancy S. Pollard. Synthesizing physically realistic human motion in low-dimensional, behavior-specific spaces. *ACM Transactions on Graphics (SIGGRAPH 2004)*, 23(3), Aug 2004.

[13] Aydin Tozeren. *Human Body Dynamics: Classical Mechanics and Human Movement*. Springer, 2000.

[14] Maurice R. Yeadon and Mark A. Brewin. Optimised performance of the backward longswing on rings. *Journal of Biomechanics*, 36:545–552, 2003.